Grey and white matter abnormalities in chronic obstructive pulmonary disease: a case-control study

Journal:	*BMJ Open*
Manuscript ID:	bmjopen-2012-000844
Article Type:	Research
Date Submitted by the Author:	12-Jan-2012
Complete List of Authors:	Zhang, Jiaxing; Department of Physiology and Neurobiology, Medical College of Xiamen University zhang, haiyan; Department of Physiology and Neurobiology, Medical College of Xiamen University, Xiamen wang, xiaochuan; Department of Neurology, the Affiliated Hospital of Hangzhou Normal University lin, Jianzhong; Magnetic Resonance Center, Zhongshan Hospital, Medical College of Xiamen University sun, Yinchuan; Department of Physiology and Neurobiology, Medical College of Xiamen University, Xiamen huang, Yongxia; Department of Physiology and Neurobiology, Medical College of Xiamen University, Xiamen yang, Tianhe; Magnetic Resonance Center, Zhongshan Hospital, Medical College of Xiamen University zheng, Shili; Departments of Respiratory, Zhongshan Hospital, Medical College of Xiamen University fan, ming; Department of Brain Protection and Plasticity, Institute of Basic Medical Sciences
Primary Subject Heading:	Radiology and imaging
Secondary Subject Heading:	Neurology
Keywords:	Adult intensive & critical care < INTENSIVE & CRITICAL CARE, Neuroradiology < NEUROLOGY, Magnetic resonance imaging < RADIOLOGY & IMAGING

Grey and white matter abnormalities in chronic obstructive pulmonary disease: a case-control study

Haiyan Zhang[1#], Xiaochuan Wang[2#], Jianzhong Lin[3], Yinchuan Sun[1], Yongxia Huang[1], Tianhe Yang[3], Shili Zheng[4], Ming Fan [5], Jiaxing Zhang*[1]

1 Department of Physiology and Neurobiology, Medical College of Xiamen University, Xiamen 361005, China;

2 Department of Neurology, the Affiliated Hospital of Hangzhou Normal University, Hangzhou 310015, China;

3 Magnetic Resonance Center, Zhongshan Hospital, Medical College of Xiamen University, Xiamen 361004, China;

4 Departments of Respiratory, Zhongshan Hospital, Medical College of Xiamen University, 361004, Xiamen, China.

5 Department of Brain Protection and Plasticity, Institute of Basic Medical Sciences, Beijing 100850, China

[#], authors with equal contributions

Corresponding author:

Jiaxing Zhang, PhD

Department of Physiology and Neurobiology

Medical College of Xiamen University

Xiamen, 361005, China

Tel: +86-0592-2188-421

Email: zhangjiaxing@xmu.edu.cn

Keywords: Brain, chronic obstructive pulmonary disease, grey matter, magnetic resonance images, white matter

Word count: 2989

ABSTRACT

Objectives The irreversible airflow limitation characterized chronic obstructive pulmonary disease (COPD) causes a decrease in oxygen supply to brain. The present study was to investigate brain structural damage in COPD. Design Retrospective case-control study. Stable COPD patients and healthy volunteers were recruited. The two groups were matched in age, sex, and educational background. Setting A hospital and a number of communities: they are all located in southern Fujian province, China. Participants 25 patients and controls were collected from December 2009 to May 2011. Primary and secondary outcome measures Using voxel-based morphometry and tract-based spatial statistics based on MR images to analyze grey matter density and white matter fractional anisotropy (FA), respectively, and a battery of neuropsychological tests were performed. Results COPD patients (vs. controls) showed decreased grey matter density in the limbic and paralimbic structures, including right gyrus rectus, left precentral gyrus, bilateral anterior and middle cingulate gyri, bilateral superior temporal gyri, bilateral anterior insula extending to Rolandic operculum, bilateral thalamus/pulvinars, and left caudate nucleus. COPD patients (vs. controls) had decreased FA values in the bilateral superior corona radiata, bilateral superior and inferior longitudinal fasciculus, bilateral optic radiation, bilateral lingual gyri, left parahippocampal gyrus, and fornix. Lower FA values in these regions were associated with increased radial diffusivity and no changes of longitudinal diffusivity. COPD patients had poor performances in the Mini Mental State Examination, figure memory, and visual reproduction. GM density in some of the above regions in COPD had positive correlations with arterial blood Po_2 while negative correlations with disease duration, and also, had positive correlations with visual tasks. Conclusion We demonstrated that COPD exhibited loss of regional grey matter accompanied by impairment of white matter microstructural integrity, which was

associated with disease severity and may underlie the pathophysiological and psychological changes of COPD.

Funding: This work was supported by National Science Foundation of China (Project No. 31071041; 81171324), Bureau of Science and Technology of Hangzhou (20090833B10), and Health Bureau of Zhejiang Province (2009A168).

Competing interests: None.

Data Sharing: We agree share our data with Dryad.

Contributorship: Hanyang Zhang, Xiaochuan Wang, Jianzhong Lin

INTRODUCTION

Chronic obstructive pulmonary disease (COPD) continues to be a major cause of morbidity and mortality. It is increasingly recognized that COPD extends beyond the lung.[1] The irreversible airflow limitation characterized COPD usually develop arterial oxygen desaturation, which could subsequently result in a decrease in oxygen transport to the brain. As the central nervous system is highly oxidative, it inevitably suffers from hypoxic stress. Hypoxia during COPD has been previously proved to induce cerebral perfusion decline[2] and metabolic decreases.[3-5] Moreover, systematic inflammation[1] may also cause neuronal damage in the brain of COPD patients. In fact, in COPD patients, clinical symptoms such as neuropsychological deficits,[6] depression and anxiety,[1] and physical disability[1] have been well documented. Taken together, all these data suggest the presence of brain structural alteration. However, until now, it remains to be largely uninvestigated.

Voxel-based morphometry (VBM) and Tract-Based Spatial Statistics (TBSS)[7] based on magnetic resonance images (MRI) were adopted to measure grey matter (GM) density and white matter (WM) fibrous microstructure properties in tracts, respectively. VBM is an automatic quantitative volumetric technique over the whole brain using voxel by voxel analysis without prior specification of regions of interest for analysis and it does not rely on arbitrarily predefined structures. Recently, the preprocessing steps of VBM have been improved with the Diffeomorphic Anatomical Registration Through Exponentiated Lie algebra (DARTEL) registration method,[8] which can achieve more accurate inter-subject registration of brain images. TBSS is a recently introduced method, which uses diffusion tensor MR imaging (DTI) to measure fractional anisotropy (FA). TBSS increases the sensitivity and the interpretability of the results compared with voxel-based approaches based purely on non-linear registration.[7] Moreover, diffusion tensor eigenvalues (longitudinal and radial diffusivities) were also

included in the analysis since they can help interpret FA changes in WM tracts by providing information regarding likely alterations in the proportion of longitudinally vs. obliquely aligned myelinated fibers. The VBM and TBSS methods have been extensively applied in clinical researches, including the evaluation of morphological characteristics of high-altitude residents in our previous study.[9]

Dyspnea is the most common complaint and most disabling symptom in patients with COPD. Functional MRI studies on breathlessness, air hunger, and inspiratory loaded breathing have revealed that a large number of brain regions, including the frontal cortex, parietal cortex, temporal cortex, limbic cortex (insular cortex, cingulate cortex, thalamus, amygdala, hippocampus, and caudate nucleus), cerebellar cortex, and brainstem, were activated by dyspnea.[10] These dyspnea-activated brain regions have been shown to be impaired in patients with congenital central hypoventilation syndrome,[11] in patients with obstructive sleep apnea patients,[12] and in high-altitude residents.[9] We therefore hypothesized that COPD patients would have similar cerebral impairment.

METHODS

Subjects

Twenty-five patients were collected from December 2009 to May 2011. All patients had undergone a period 30 to 45 days of in-hospital rehabilitation following an acute exacerbation of COPD. At the time of data collection, patients were in stable condition. Among these patients, 12 discharged patients were recruited during their rest at home and 13 patients were recruited when they were awaiting discharge from hospital. Patients were diagnosed in Zhongshan hospital (Xiamen, China) according to the diagnostic criteria of Global Initiative for Chronic Obstructive Lung Disease (GOLD).[13] Twenty-five

healthy volunteers, with comparable age, sex, and educational background, comprised the control group. All the subjects were free from a known history of cerebrovascular accident, heart failure, neurological disorders, OSA, or other diseases known to affect cognition. Patients were provided with therapy including inhaled ipratropium bromide, bricanyl, ventoline, and budesonide. Demographic characteristics of the patients and healthy volunteers were listed in Table 1. Procedures were fully explained and all subjects were provided written informed consent before participating in the study. The experimental protocol was approved by the Research Ethics Review Board of Xiamen University.

Physiological and neuropsychological tests

Physiological and neuropsychological tests and activities of daily living (ADL) (score range 14-56)[14] were conducted one day before MRI scan. The neuropsychological tests include: (i) the Chinese version of the Mini Mental State Examination (MMSE) measured the general cognitive function. (ii) the visual reproduction test, figure memory test, and digital span forward and backward tasks from the Chinese revised version of Wechsler Memory Scale measured visual construction ability, visuospatial memory, and short-term working memory, respectively. All data were analyzed using SPSS 19.0 (Chicago, IL, USA). Independent t test measures between-group differences.

MRI data acquisition

Images were acquired on a Siemens Trio Tim 3.0T (Erlangen, Germany) at MRI Research Center (Zhongshan Hospital, Xiamen, China). A 3D structural MRI was acquired from each subject using a T1-weighted MPRAGE sequence (TR/TE = 1900 ms/2.48 ms, FOV = 25 × 25 cm^2, NEX = 1, matrix = 512 × 256, slice thickness = 1.0 mm). Conventional 2D T1 and T2 images were also acquired and

examined for any incidental findings. A DTI pulse sequence with single shot diffusion-weighted echo planar imaging (TR/TE = 3600/95 ms, FOV=24 × 24 cm^2, NEX = 2, matrix = 128 × 128, slice thickness = 4.5 mm) was applied sequentially in 30 non-collinear directions (b-value = 1000s/ mm^2) with one scan without diffusion weighting (b = 0s/mm^2). The following data analyses were conducted by two researchers who were blind to the status of subjects.

VBM analysis of 3D T1 images

The 3D T1 images were used for GM analysis using VBM8 toolbox implemented in SPM8 (Wellcome Department of Imaging Neuroscience, University College London, London, UK). The following processing steps were carried out: (i) the images were inspected and set at the anterior commissure. Each reorientated image was segmented into GM, WM and CSF in native space and procrustes aligned GM images were generated by a rigid transformation. (ii) the DARTEL was used to create study-specific template by the aligned images from all the patients and controls to improve inter-subject registration of structural images.[8] The procedure implicated in six iterations, which began with the averaging of aligned data to generate an original template. Then, the first iteration of the registration was done on each subject and a new template was created. After this, the second iteration began. When six iterations were finished, the template was generated, which was the average of the DARTEL registered data. During iterations, all images were warped to the template yielding a series of flow fields that parameterized deformations. (iii) the normalized images were transformed into MNI space. These GM images were then smoothed using a Gaussian kernel of 8 mm full-width at half-maximum. Independent t-tests were performed to examine between-group differences. The statistical parametric map was generated with threshold at $t > 3.7734$, $p < 0.01$ (FDR correction with

sex, age, education, and total intracranial volume as covariates).

TBSS analysis of DTI

DCM2MII was used to convert diffusion tensor images from the proprietary scanner format to the NIFTI format. Then images were processed using FSL 4.1.5 software package (http://www.fmrib.ox.ac.uk/fsl/). Images were realigned to the b-value (b0) image to remove eddy current distortions and motion artifacts using FMRIB's diffusion toolbox (FDT).[15] Brain mask was created from the first b0 image using Brain Extraction Tool (BET). After these processes images were calculated with the FDT for FA, longitudinal diffusivity (principal diffusion direction, $\lambda 1$) and radial diffusivity (transverse diffusion component, $[(\lambda 2+\lambda 3)/2]$) maps. The analysis of FA images was performed using TBSS in FSL.[7] TBSS processing includes the following steps: (i) align the FA images of all subjects to a template which was arbitrarily selected from those FA images by nonlinear registrations; (ii) transform all the aligned FA images into $1\times1\times1$ mm^3 MNI152 space by affine registrations; (iii) create the mean FA image and filter to retain only the center of the WM tracts so as to create the mean FA skeleton. (iv) project individual subjects' FAs onto mean FA skeleton. (v) following these steps, data were fed into voxel-wise cross-subject statistical analyses. In all cases, the null distribution was built up over 5000 permutations, with significance analyzed using independent t-tests at $p < 0.05$ levels, uncorrected for multiple comparisons. We determined the anatomic localization of each cluster by means of the FSL atlas tool, which incorporates several anatomic templates, including the Harvard-Oxford Cortical Structural Atlas, Harvard-Oxford Subcortical Structural Atlas, Talairach Daemon Labels, and MNI Structural Atlas.

Within the cluster of changed FA, $\lambda 1$ and $(\lambda 2+\lambda 3)/2$ were calculated. Data were analyzed using

SPSS. ANOVA statistic identified the differences between groups. Statistical significance was set at $p < 0.05$.

RESULTS

Physiological and behavioral findings

Compared with the controls, COPD patients had significant decreases in arterial blood Sao_2 ($p = 0.003$) and Po_2 ($p = 0.006$), and increases in arterial blood Pco_2 ($p < 0.001$) and heart rate ($p < 0.001$). Pulmonary function test showed that COPD patients had significant lower one second over forced vital capacity (FVC), forced expiratory volume (FEV), and FEV1/FVC value (all, $p < 0.001$) and higher respiratory rate ($p = 0.003$) compared with the controls.

Compared with the controls, COPD patients had significant lower scores in ADL ($p < 0.001$), MMSE test ($p < 0.001$), visual reproduction ($p = 0.031$), and figure memory ($p = 0.01$). No significant differences were found in the other behavioral tests between the COPD patients and controls.

GM density

No subject from either group showed visible abnormalities on T1-weighted structural images. VBM analysis showed that COPD patients had decreased GM density compared with healthy controls in the right gyrus rectus, left precentral gyrus, bilateral anterior and middle cingulate gyri, bilateral superior temporal gyri, bilateral anterior insula extending to Rolandic operculum (base of the pre- and post-central gyri), bilateral thalamus/pulvinars, and left caudate nucleus (cluster size > 100 voxels) (Fig. 1, Fig. 2, Fig. 3, Fig. 4, Table 2).

FA, longitudinal diffusivity, and radial diffusivity in relation to COPD

Whole brain voxel-wise statistic analysis showed COPD patients had significantly lower FA in a broad range of brain regions compared with controls (Fig. 5, Table 3). The significantly affected regions (clusters size > 40 voxels) included the superior corona radiata (corresponding to bilateral precuneus and bilateral superior parietal lobules), superior longitudinal fasciculus (bilateral supramarginal gyri), inferior longitudinal fasciculus (left superior temporal gyrus, right middle temporal gyrus, and fusiform gyrus), bilateral optic radiation, bilateral lingual gyri, left parahippocampal gyrus, and fornix.

Lower FA values in these regions were associated with increased radial diffusivity and no changes of longitudinal diffusivity in COPD patients vs. controls (Table 3).

Correlations between MRI measurement and disease severity

The correlations were listed in Table 4. In COPD patients, partial correlation (controlling for disease duration, FEV1/FVC, and age) revealed GM density in the bilateral anterior cingulate cortex, left superior temporal cortex, bilateral insula/superior temporal/Rolandic Operulum, bilateral thalamus/Pulvinar, and left caudate nucleus had positive correlations with arterial blood Po_2. Partial correlation (controlling for Po_2, FEV1/FVC, and age) revealed GM density in the bilateral anterior cingulated cortex, right insula/superior temporal/Rolandic Operulum, and right thalamus/Pulvinar had negative correlations with disease duration. The GM density in the left superior temporal lobes and left insula/superior temporal/Rolandic Operculum in COPD patients was significantly correlated with figure memory score. The GM density in left precentral gyrus and left thalamus/Pulvinar in COPD patients was significantly correlated with visual reproduction.

DISCUSSION

Our present study revealed that COPD patients had decreased regional GM density confined to the limbic and paralimbic structures. GM density in impaired regions in COPD patients had significant positive correlation with arterial blood Po_2 and negative correlation with disease duration. The decreased WM FA value with increased radial diffusivity value was detected mainly in the visual cortex of occipital lobe, the posterior parietal lobe as well as the temporal lobe. Decreased FA was associated with compromised myelin structure, changes in axonal morphologic structure, and altered interaxonal spacing of fiber bundles.[16] Radial diffusivity measures motion of water molecules perpendicular to fibers and increase of radial diffusivity is interpreted as abnormalities in myelinated membranes.[17] Consequently, decreased FA and increased diffusivity in COPD indicated the impairment of WM microstructural integrity.

Impaired brain regions are implicated in other subjects suffered from hypoxia

The impaired brain regions in COPD have also been found in other chronic hypoxic diseases. For example, decrease of GM volume/concentration in the gyrus rectus, precentral gyrus, anterior cingulate cortex, multiple sites within the temporal lobes, insular cortex, thalamus, and caudate nucleus were detected in patients with obstructive sleep apnea.[12] Impairments of WM microstructure in the temporal lobe, parietal lobe, fornix, and corona radiata were found in patients with congenital central hypoventilation syndrome.[11] In our previous study, the decrease of GM volume in the anterior insula, anterior cingulate cortex, and precentral cortex were found on high-altitude residents.[9]

The mechanisms involved in the morphological impairments

GM density in impaired regions in COPD patients had strongly positive correlation with the arterial blood Po_2, which suggested the impairment in GM may result from low blood oxygen. Moreover, the GM density in some impaired regions showed negative correlations with disease duration, suggesting the more GMs were lost with low oxygen persists. It is already known that hypoxia can induce metabolic decreases[3-5] and cerebral perfusion decline[2] in COPD. In addition, COPD patients often suffer from systemic inflammation, which can exacerbate neuronal injury.[1] A greater proportion of regions showing GM loss located in limbic/paralimbic cortex in COPD patients may be due to that those phylogenetically older regions of the brain showed sharper vascular responses to hypoxia than evolutionary younger regions.[18]

Morphological impairments play a role in respiratory and cardiovascular responses to dyspnea and hypoxia

Impairment in anterior insula and anterior cingulate cortex could play a role in perception of air hunger. Various breath control tasks have shown these regions are the components of a larger cortical network underlying the perception of dyspnea, and among all structures, the anterior insular cortex is suggested to be an especially crucial brain region.[10] Moreover, the right insular lesions patients showed reduce in perception of dyspnea.[19] Posterior thalamus has been previously implicated in suppressing the ventilatory response to hypoxia. Lesions in posterior thalamus abolish hypoxia-induced inhibition of fetal breathing movements while local electrical stimulation effectively decreases respiratory frequency.[20] Thus the impaired GM in posterior thalamus may clarify the enhanced breathing movements in COPD patients.

Human studies have shown a central autonomic network made up of limbic systems including the

insular cortex and anterior cingulate gyrus play an important role in regulating the cardiovascular system.[21] Microinjection of opiates into the hippocampus reduced arterial pressure and heart rate, and the destruction of opiate-producing hippocampal neurons increased blood pressure.[22] Hippocampus has indirect projections to sympathetic targets, including the adrenal gland and satellite ganglion. The fornix is the main input and output pathway of the hippocampus. Therefore, decreased GM or impaired WM in these areas may elucidate cardiovascular disturbances in COPD patients.[1]

Morphological impairments contribute to cognitive deficits

In the present study, COPD patients had poorer performance in MMSE, visuospatial memory, and visual construction task. These results were consistent with that found in previous studies in COPD patients.[6] In line with the present findings in COPD, we previously found that long-time living at mild high-altitude hypoxic environment impaired cognitive performances only confined to visual reproduction and short-time complex figure memory.[23] In our present study, the decreases of GM density in frontal precentral cortex, insula/superior temporal cortex/Rolandic Operculum, and thalamus/pulvinar may be responsible for the deficit in visual-related tasks since the GM density in these areas showed a significantly positive correlation with figure memory or visual reproduction score. The following previous data may support our findings: (i) Recent research has identified the inferior frontal cortex served as a source of top-down modulation underlying attention to visual features.[24] (ii) Studies on patients using fMRI and PET demonstrated Rolandic operculum as one of the visual structures.[25] (iii) The pulvinar region of the thalamus is known to project to posterior parietal lobe and inferior temporal lobe. The pulvinar nucleus of the thalamus together with anterior cingulate cortex and posterior parietal lobe constitutes a network control visual attention.[26] The pulvinar has been implicated

in various visual functions in lesion studies.[27]

Our present study found the impairments of WM limited to the pathways of visual processing, including optic radiation, posterior parietal lobe (superior parietal lobule, supramarginal gyrus, and precuneus), and the inferior temporal fusiform and lingual gyri. Visual information enters the primary visual cortex via optic radiation to the visual cortex. Cortical areas along the posterior parietal 'dorsal stream' are primarily concerned with spatial localization and directing attention, while cortical areas along the inferior temporal 'ventral stream' are mainly concerned with the recognition and identification of visual stimuli.[28] COPD also showed impaired WM in middle temporal gyrus. Middle temporal cortex is important for the long-term buildup of perceptual memory for ambiguous motion stimuli.[29] Based on the above data, our findings in WM may also clarify the mechanisms underling the deficit in visual-related tasks. In addition, impaired WM in input and output fibers of hippocampus (fornix) may be related to the deficit in MMSE. Previous study on patients with Alzheimer's disease found the volumes of hippocampus were significantly reduced and the volumes of the left hippocampus correlated significantly with the MMSE score.[30] The limitation of our study is the weak statistical power of FA value analysis, because the results obtained in the TBSS analysis could not survive multiple comparison correction.

Morphological impairments contribute to the depression

Several researches revealed that depression involved the dorsal prefrontal cortices, anterior cingulate cortex, and the basal ganglia.[31] Insular cortex played an important role in anxiety disorders through its mediation of interoceptive processing.[32] Decreased bilateral lingual gyrus and caudate nucleus volume were found in major depression.[33,34] The connections of thalamus with prefrontal

cortico-striato-pallidus loop and amygdalo-striato-pallidus loop have been implicated in mood disorders.[35] Taken together, the loss of GM in these structures possibly contributes to mood symptoms of COPD.[1]

Conclusions

In summary, we first demonstrated that COPD extended beyond the lung to the brain, with the decrease of regional GM density accompanied by impairment in the WM microstructural integrity. Our findings suggest significant participation of these structures in responding to hypoxic challenges, which include cardiovascular and air-hunger components. The brain structural changes may also underlie the psychological and mood changes of COPD.

Authors' contributions

Haiyan Zhang: contributed to the study design, take responsibility for the integrity of the data, the accuracy of the data analysis.

Xiaochuan Wang: contributed to the study design, collection, analysis, and interpretation of data, and critical review.

Jianzhong Lin: contributed to the collection, analysis, and interpretation of data.

Yingchun Sun: contributed to the collection, analysis, and interpretation of data.

Yongxia Huang: contributed to the collection, analysis, and interpretation of data.

Tianhe Yang: contributed to the collection, analysis, and interpretation of data.

Shili Zheng: contributed to the collection, analysis, and interpretation of data.

Ming Fan: contributed to the study design, drafting, critical review, and final approval of the

manuscript.

Jiaxing Zhang: contributed to conception and design, interpretation of data, drafting the article, and final approval of the manuscript.

Table 1 Demographic characteristics of the patients with COPD and healthy volunteers

	COPD patients	Controls	p
Number of subjects	25	25	
Gender (female) (%)	16	16	
Age (years) (mean ± SD)	69.2 ± 8.1 (58 - 84)	67.96 ± 8.0 (57 - 86)	0.59
Education (years) (mean ± SD)	6.7 ± 3.9	7.5 ± 5.0	0.53
Family history of COPD (%)	4	-	
Disease duration (years)	7.0 ± 5.7	-	
Actual smokers (%)	44	40	0.86

Table 2 Regional information of decreased grey matter density (cluster size > 100 voxels) in COPD patients compared with healthy controls

Area	Volume (mm^3)	Brodmann areas	MNI coordinate			t-score (peak)
			x	y	z	
Rectus_R	118	11	9	39	-20	4.31
Precentral_L	100	6	-51	-5	33	4.95
Cingulum_Ant_R	485	32	8	38	17	5.88
Cingulum_Ant_L	212	32	-8	38	18	4.49
Cingulum_Mid_R	157	24	6	-9	42	4.87
Cingulum_Mid_L	136	24	-6	-9	41	4.91
Temporal_Sup_ L	280	22/42	-60	-33	3	4.99
Temporal_Sup/ Rolandic_Oper _L	837	22	-57	-14	10	4.91
Insula/Temporal_Sup/ Rolandic_Oper _R	2821	13/22/47	44	11	-5	5.15
Insula/Temporal_Sup/ Rolandic_Oper _L	1551	13/22/47	-33	12	-15	4.48
Thalamus/Pulvinar_L	1270		-12	-30	3	6.46
Thalamus/Pulvinar_R	2210		12	-26	8	5.29
Caudate_L	212		-9	14	14	4.19

Table 3 Main regions showing FA, λ1, λ23 values in COPD patients compared with healthy controls

MNI (peak)			Voxels	White matter	Corresponding cortical area	FA value		λ1 (×10^3 mm^2/s)		λ23 (×10^3 mm^2/s)	
x	y	z	(mm^3)	tract		COPD	Control	COPD	Control	COPD	Control
1	10	16	240	Fornix	Fornix	0.248(0.067)	0.289(0.073)	2.586(0.314)	2.406(0.0321)	1.809(0.295)	1.577(0.262)*
-26	-69	1	191	Lingual gyrus	Left lingual gyrus	0.259(0.042)	0.283(0.046)	1.450(0.240)	1.370(0.224)	0.992(0.185)	0.896(0.168)*
27	-53	3	147	Lingual gyrus	Right lingual gyrus	0.265(0.065)	0.290(0.056)	1.381(0.239)	1.346(0.227)	0.955(0.242)	0.891(0.215)*
-23	-19	-24	77	Parahippocampus	Left parahippocampus	0.268(0.042)	0.319(0.046)	1.234(0.057)	1.189(0.052)	0.869(0.148)	0.771(0.125)*
38	-24	-24	77	fusiform gyrus	Right fusiform gyrus	0.231(0.037)	0.248(0.046)	1.053(0.063)	1.094(0.073)	0.774(0.030)	0.723(0.032)*
-10	-91	17	204	Optic radiation	Left occipital cortex	0.234(0.043)	0.277(0.041)	1.037(0.038)	1.020(0.031)	0.752(0.063)	0.693(0.051)*
25	-86	-5	200	Optic radiation	Right occipital cortex	0.369(0.099)	0.409(0.122)	1.171(0.014)	1.177(0.171)	0.649(0.057)	0.601(0.071)*
-9	-72	45	94	SCR	Left precuneus	0.283(0.053)	0.317(0.056)	1.099(0.032)	1.069(0.041)	0.726(0.075)	0.665(0.065)*
9	-66	37	57	SCR	Right precuneus	0.251(0.030)	0.280(0.044)	1.044(0.032)	1.018(0.023)	0.868(0.073)	0.731(0.084)*
-15	-51	62	57	SCR	Left superior parietal lobule	0.267(0.043)	0.294(0.043)	1.130(0.051)	1.082(0.025)	0.724(0.039)	0.671(0.045)*
16	-45	64	66	SCR	Right superior parietal lobule	0.251(0.043)	0.294(0.051)	1.176(0.117)	1.107(0.094)	0.805(0.056)	0.762(0.056)*
-45	-53	31	44	SLF	Left supramarginal gyrus	0.221(0.027)	0.239(0.026)	1.088(0.020)	1.076(0.040)	0.935(0.090)	0.873(0.071)*
37	-68	21	63	SLF	Right supramarginal gyrus	0.220(0.025)	0.237(0.025)	1.116(0.039)	1.090(0.052)	0.773(0.076)	0.715(0.007)*
-48	0	-16	43	ILF	Left superior temporal gyrus	0.244(0.013)	0.270(0.021)	1.060(0.030)	0.984(0.015)	0.758(0.025)	0.714(0.037)*
53	-46	-6	41	ILF	Right middle temporal gyrus	0.206(0.016)	0.241(0.024)	1.025(0.016)	1.006(0.021)	1.605(0.167)	1.340(0.139)*

ILF, inferior longitudinal fasciculus; SCR, superior corona radiata; SLF, superior longitudinal fasciculus. Data are presented as means (SD). *p<0.05.

Table 4 Correlations of grey matter density in impaired regions with Po_2, disease duration, and cognitive performances in patients with COPD

Area	Po_2	Disease duration	Cognitive performances	
			figure memory	visual reproduction
Precentral_L				r=0.503, p=0.048
Cingulum_Ant_R	r=0.530, p=0.017	r=-0.524, p=0.019		
Cingulum_Ant_L	r=0.744, p <0.001	r=-0.531, p=0.017		
Cingulum_Mid_R				
Cingulum_Mid_L				
Temporal_Sup_L	r=0.681, p=0.002		r=0.642, p=0.012	
Temporal_Sup/ Rolandic_Oper_L				
Insula/Temporal_Sup/Rolandic_Oper_R	r=0.559, p=0.012	r=-0.528, p=0.018		
Insula/Temporal_Sup/Rolandic_Oper_L	r=0.570, p=0.011		r=0.585, p=0.023	
Thalamus/Pulvinar_L	r=0.476, p =0.031			r=0.520, p =0.042
Thalamus/Pulvinar_R	r=0.499, p =0.024	r=-0.533, p=0.017		
Caudate_L	r=0.541, p=0.015			

REFERENCES

1. Barnes PJ. Chronic obstructive pulmonary disease: effects beyond the lungs. *PLoS Med* 2010; 7:e1000220.
2. Ortapamuk H, Naldoken S. Brain perfusion abnormalities in chronic obstructive pulmonary disease: comparison with cognitive impairment. *Ann Nucl Med* 2006; 20:99-106.
3. Shim TS, Lee JH, Kim SY, *et al*. Cerebral metabolic abnormalities in COPD patients detected by localized proton magnetic resonance spectroscopy. *Chest* 2001; 120:1506-13.
4. Sicard KM, Duong TQ. Effects of hypoxia, hyperoxia, and hypercapnia on baseline and stimulus-evoked BOLD, CBF, and CMRO2 in spontaneously breathing animals. *Neuroimage* 2005; 25:850-8.
5. Sinha S, Kumar V, Jagannathan NR, *et al*. Proton magnetic resonance spectroscopy of brain to study the cerebral metabolic abnormalities in COPD patients: a case control study in north India. *Indian J Chest Dis Allied Sci* 2009; 51:15-9.
6. Dodd JW, Getov SV, Jones PW. Cognitive function in COPD. *Eur Respir J* 2010; 35:913-22.
7. Smith SM, Jenkinson M, Johansen-Berg H, *et al*. Tract-based spatial statistics: voxelwise analysis of multi-subject diffusion data. *Neuroimage* 2006; 31:1487-505.
8. Ashburner J. A fast diffeomorphic image registration algorithm. *Neuroimage* 2007; 38:95-113.
9. Zhang J, Yan X, Shi J, *et al*. Structural modifications of the brain in acclimatization to high-altitude. *PLoS One* 2010; 5:e11449.
10. von Leupoldt A, Dahme B. Cortical substrates for the perception of dyspnea. *Chest* 2005; 128:345-54.
11. Kumar R, Macey PM, Woo MA, *et al*. Diffusion tensor imaging demonstrates brainstem and

cerebellar abnormalities in congenital central hypoventilation syndrome. *Pediatr Res* 2008; 64:275-80.

12. Joo EY, Tae WS, Lee MJ, *et al*. Reduced brain gray matter concentration in patients with obstructive sleep apnea syndrome. *Sleep* 2010; 33:235-41.
13. Pauwels RA, Buist AS, Calverley PM, *et al*. Global strategy for the diagnosis, management, and prevention of chronic obstructive pulmonary disease. NHLBI/WHO Global Initiative for Chronic Obstructive Lung Disease (GOLD) Workshop summary. *Am J Respir Crit Care Med* 2001; 163:1256-76.
14. Lawton MP, Brody EM. Assessment of older people: self-maintaining and instrumental activities of daily living. *Gerontologist* 1969; 9:179-86.
15. Jenkinson M, Smith S. A global optimisation method for robust affine registration of brain images. *Med Image Anal* 2001; 5:143-56.
16. Beaulieu C. The basis of anisotropic water diffusion in the nervous system - a technical review. *NMR Biomed* 2002; 15:435-55.
17. Song SK, Sun SW, Ramsbottom MJ, *et al*. Dysmyelination revealed through MRI as increased radial (but unchanged axial) diffusion of water. *Neuroimage* 2002; 17:1429-36.
18. Binks AP, Cunningham VJ, Adams L, *et al*. Gray matter blood flow change is unevenly distributed during moderate isocapnic hypoxia in humans. *J Appl Physiol* 2008; 104:212-7.
19. Schon D, Rosenkranz M, Regelsberger J, *et al*. Reduced perception of dyspnea and pain after right insular cortex lesions. *Am J Respir Crit Care Med* 2008; 178:1173-7.9.
20. Teppema LJ, Dahan A. The ventilatory response to hypoxia in mammals: mechanisms, measurement, and analysis. *Physiol Rev* 2010; 90:675-754.

21. Nagai M, Hoshide S, Kario K. The insular cortex and cardiovascular system: a new insight into the brain-heart axis. *J Am Soc Hypertens* 2010; 4:174-82.

22. Macefield VG, Gandevia SC, Henderson LA. Neural sites involved in the sustained increase in muscle sympathetic nerve activity induced by inspiratory capacity apnea: a fMRI study. *J Appl Physiol* 2006; 100:266-73.

23. Zhang J, Liu H, Yan X, *et al*. Minimal effects on human memory following long-term living at moderate altitude. *High Alt Med Biol* 2011; 12:37-43.

24. Zanto TP, Rubens MT, Bollinger J, *et al*. Top-down modulation of visual feature processing: the role of the inferior frontal junction. *Neuroimage* 2010; 53:736-45.

25. Fried I, Nenov VI, Ojemann SG, *et al*. Functional MR and PET imaging of rolandic and visual cortices for neurosurgical planning. *J Neurosurg* 1995; 83:854-61.

26. Heinze HJ, Mangun GR, Burchert W, *et al*. Combined spatial and temporal imaging of brain activity during visual selective attention in humans. *Nature* 1994; 372:543-6.

27. Arend I, Machado L, Ward R, *et al*. The role of the human pulvinar in visual attention and action: evidence from temporal-order judgment, saccade decision, and antisaccade tasks. *Prog Brain Res* 2008; 171:475-83.

28. Itti L, Koch C. Computational modelling of visual attention. *Nat Rev Neurosci* 2001; 2:194-203

29. Brascamp JW, Kanai R, Walsh V, *et al*. Human middle temporal cortex, perceptual bias, and perceptual memory for ambiguous three-dimensional motion. *J Neurosci* 2010; 30:760-6.

30. Laakso MP, Soininen H, Partanen K, *et al*. Volumes of hippocampus, amygdala and frontal lobes in the MRI-based diagnosis of early Alzheimer's disease: correlation with memory functions. *J Neural Transm Park Dis Dement Sect* 1995; 9:73-86.

31. Canbeyli R. Sensorimotor modulation of mood and depression: an integrative review. *Behav Brain Res* 2010; 207:249-64.

32. Stein MB, Stein DJ. Social anxiety disorder. *Lancet* 2008; 371:1115-25.

33. Veer IM, Beckmann CF, van Tol MJ, *et al*. Whole brain resting-state analysis reveals decreased functional connectivity in major depression. *Front Syst Neurosci* 2010; 4: 41.

34. Baumann B, Danos P, Krell D, *et al*. Reduced volume of limbic system-affiliated basal ganglia in mood disorders: preliminary data from a postmortem study. *J Neuropsychiatry Clin Neurosci* 1999; 11:71-8.

35. Price JL, Drevets WC. Neurocircuitry of mood disorders. *Neuropsychopharmacology* 2010; 35:192-216.

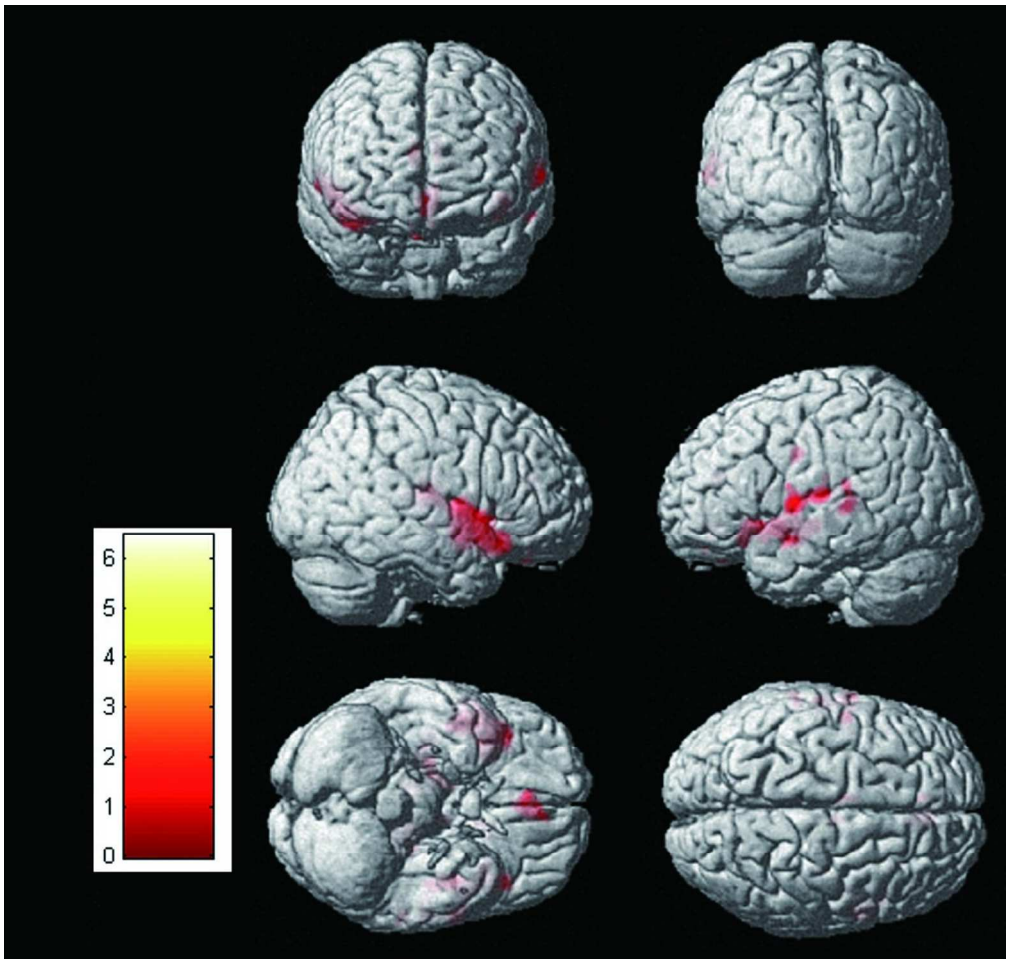

Figure 1 A statistical parametric map for grey matter density reduced in COPD patients vs. healthy controls (pFDR_corrected< 0.01) overlaid on the MNI template.

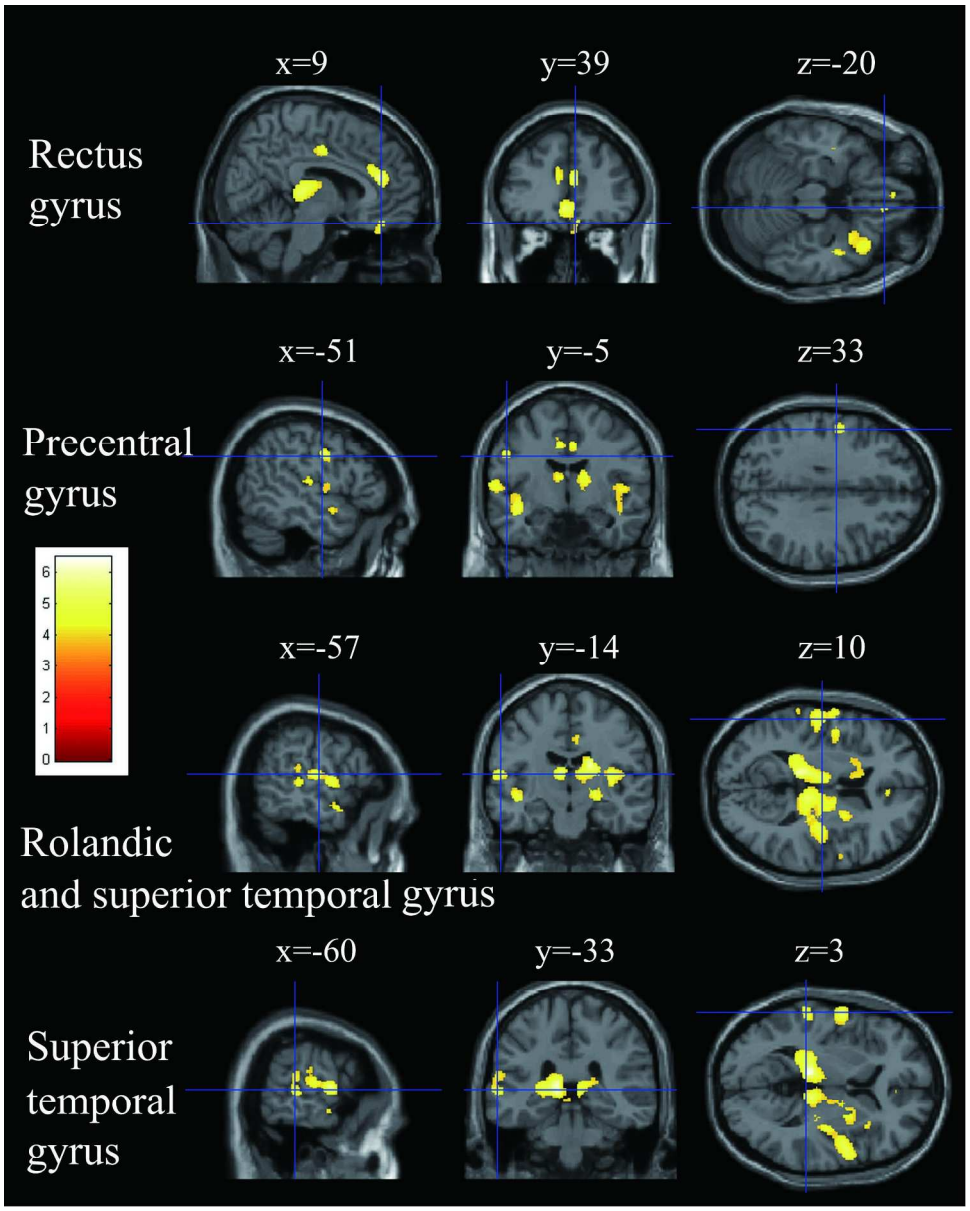

Figure 2 Grey matter density decrease in COPD patients vs. healthy controls. Three-dimensional slices depicting regions showing reduced grey matter in the right gyrus rectus, left precentral gyrus, left Rolandic operculum and superior temporal gyrus overlaid on a T1-weighted MRI anatomical image in the MNI template.

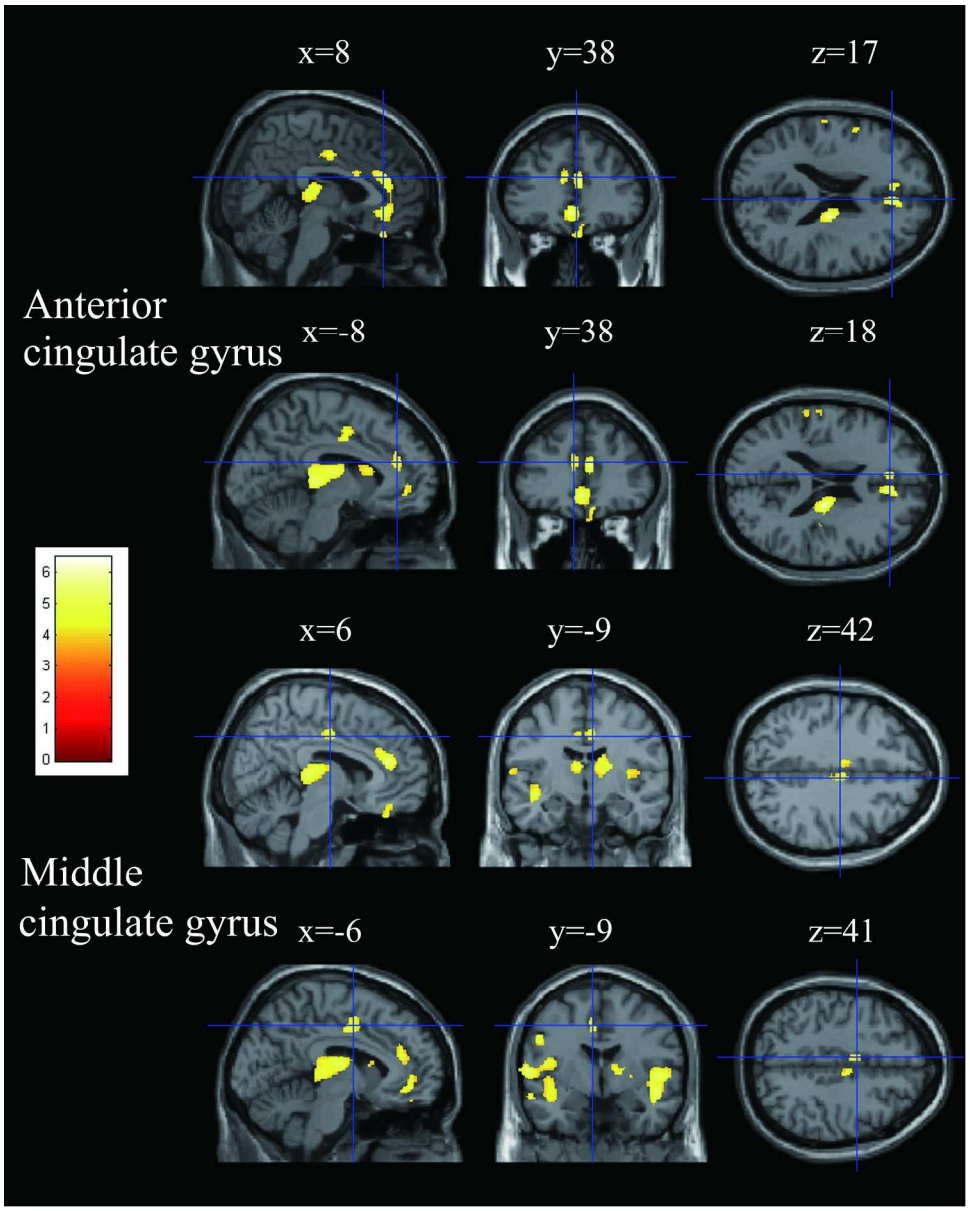

Figure 3 Grey matter density decrease in COPD patients vs. healthy controls. Three-dimensional slices depicting regions showing reduced grey matter in the bilateral anterior and middle cingulate gyri overlaid on a T1-weighted MRI anatomical image in the MNI template.

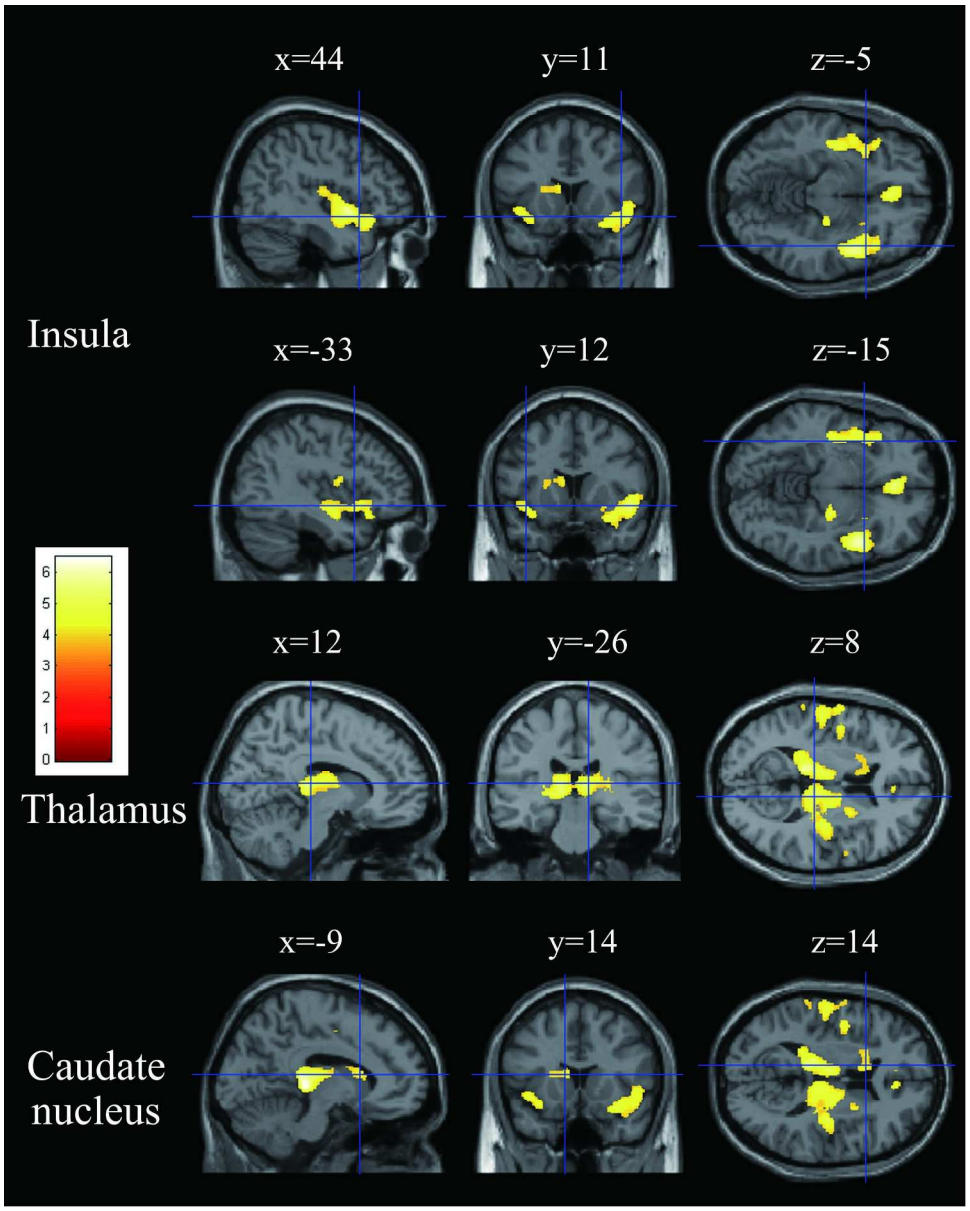

Figure 4 Grey matter density decrease in COPD patients vs. healthy controls. Three-dimensional slices depicting regions showing reduced grey matter in the bilateral insula, bilateral thalamus, and left caudate nucleus overlaid on a T1-weighted MRI anatomical image in the MNI template.

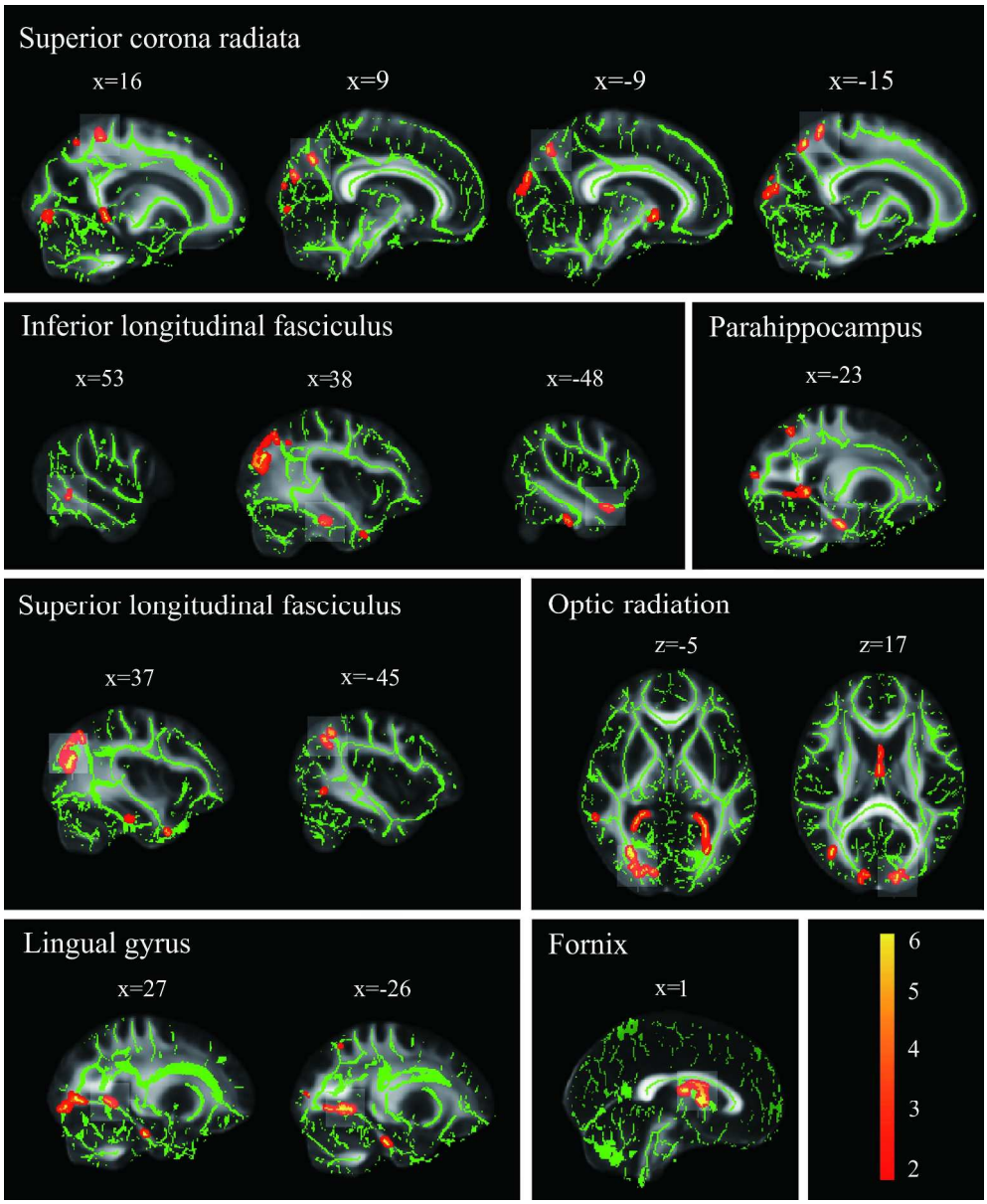

Figure 5 Statistical maps of group comparison of FA value on a voxel-wise basis (results of TBSS). The group's mean FA skeleton (green) was overlaid on the MNI template. The threshold of mean FA skeleton was set at 0.2. COPD patients show significantly lower FA value than healthy controls ($p < 0.05$).

STROBE 2007 (v4) Statement—Checklist of items that should be included in reports of *case-control studies*

Section/Topic	Item #	Recommendation	Reported on page #
Title and abstract	1	(*a*) Indicate the study's design with a commonly used term in the title or the abstract	1
		(*b*) Provide in the abstract an informative and balanced summary of what was done and what was found	2
Introduction			
Background/rationale	2	Explain the scientific background and rationale for the investigation being reported	4
Objectives	3	State specific objectives, including any prespecified hypotheses	4 and 5
Methods			
Study design	4	Present key elements of study design early in the paper	5
Setting	5	Describe the setting, locations, and relevant dates, including periods of recruitment, exposure, follow-up, and data collection	5
Participants	6	*(*a) Give the eligibility criteria, and the sources and methods of case ascertainment and control selection. Give the rationale for the choice of cases and controls	5 and 6
		(*b*) For matched studies, give matching criteria and the number of controls per case	5
Variables	7	Clearly define all outcomes, exposures, predictors, potential confounders, and effect modifiers. Give diagnostic criteria, if applicable	5
Data sources/ measurement	8*	For each variable of interest, give sources of data and details of methods of assessment (measurement). Describe comparability of assessment methods if there is more than one group	*6*
Bias	9	Describe any efforts to address potential sources of bias	
Study size	10	Explain how the study size was arrived at	
Quantitative variables	11	Explain how quantitative variables were handled in the analyses. If applicable, describe which groupings were chosen and why	
Statistical methods	12	(*a*) Describe all statistical methods, including those used to control for confounding	6 - 8
		(*b*) Describe any methods used to examine subgroups and interactions	6 - 8
		(*c*) Explain how missing data were addressed	
		(*d*) If applicable, explain how matching of cases and controls was addressed	
		(*e*) Describe any sensitivity analyses	6 - 8
Results			

Participants	13*	(a) Report numbers of individuals at each stage of study—eg numbers potentially eligible, examined for eligibility, confirmed eligible, included in the study, completing follow-up, and analysed	5
		(b) Give reasons for non-participation at each stage	
		(c) Consider use of a flow diagram	
Descriptive data	14*	(a) Give characteristics of study participants (eg demographic, clinical, social) and information on exposures and potential confounders	17
		(b) Indicate number of participants with missing data for each variable of interest	
Outcome data	15*	Report numbers in each exposure category, or summary measures of exposure	
Main results	16	(*a*) Give unadjusted estimates and, if applicable, confounder-adjusted estimates and their precision (eg, 95% confidence interval). Make clear which confounders were adjusted for and why they were included	9 and 10
		(*b*) Report category boundaries when continuous variables were categorized	
		(*c*) If relevant, consider translating estimates of relative risk into absolute risk for a meaningful time period	
Other analyses	17	Report other analyses done—eg analyses of subgroups and interactions, and sensitivity analyses	
Discussion			
Key results	18	Summarise key results with reference to study objectives	11
Limitations	19	Discuss limitations of the study, taking into account sources of potential bias or imprecision. Discuss both direction and magnitude of any potential bias	
Interpretation	20	Give a cautious overall interpretation of results considering objectives, limitations, multiplicity of analyses, results from similar studies, and other relevant evidence	11-15
Generalisability	21	Discuss the generalisability (external validity) of the study results	
Other information			
Funding	22	Give the source of funding and the role of the funders for the present study and, if applicable, for the original study on which the present article is based	3

*Give information separately for cases and controls in case-control studies and, if applicable, for exposed and unexposed groups in cohort and cross-sectional studies.

Note: An Explanation and Elaboration article discusses each checklist item and gives methodological background and published examples of transparent reporting. The STROBE checklist is best used in conjunction with this article (freely available on the Web sites of PLoS Medicine at http://www.plosmedicine.org/, Annals of Internal Medicine at http://www.annals.org/, and Epidemiology at http://www.epidem.com/). Information on the STROBE Initiative is available at www.strobe-statement.org.

Grey and white matter abnormalities in chronic obstructive pulmonary disease: a case-control study

Journal:	*BMJ Open*
Manuscript ID:	bmjopen-2012-000844.R1
Article Type:	Research
Date Submitted by the Author:	14-Feb-2012
Complete List of Authors:	zhang, haiyan; Department of Physiology and Neurobiology, Medical College of Xiamen University, Xiamen wang, xiaochuan; Department of Neurology, the Affiliated Hospital of Hangzhou Normal University lin, Jianzhong; Magnetic Resonance Center, Zhongshan Hospital, Medical College of Xiamen University sun, Yinchuan; Department of Physiology and Neurobiology, Medical College of Xiamen University, Xiamen huang, Yongxia; Department of Physiology and Neurobiology, Medical College of Xiamen University, Xiamen yang, Tianhe; Magnetic Resonance Center, Zhongshan Hospital, Medical College of Xiamen University zheng, Shili; Departments of Respiratory, Zhongshan Hospital, Medical College of Xiamen University fan, ming; Department of Brain Protection and Plasticity, Institute of Basic Medical Sciences Zhang, Jiaxing; Department of Physiology and Neurobiology, Medical College of Xiamen University
Primary Subject Heading:	Radiology and imaging
Secondary Subject Heading:	Neurology
Keywords:	Adult intensive & critical care < INTENSIVE & CRITICAL CARE, Neuroradiology < NEUROLOGY, Magnetic resonance imaging < RADIOLOGY & IMAGING

Grey and white matter abnormalities in chronic obstructive pulmonary disease: a case-control study

Haiyan Zhang[1#], Xiaochuan Wang[2#], Jianzhong Lin[3], Yinchuan Sun[1], Yongxia Huang[1], Tianhe Yang[3], Shili Zheng[4], Ming Fan [5], Jiaxing Zhang*[1]

1 Department of Physiology and Neurobiology, Medical College of Xiamen University, Xiamen 361005, China;

2 Department of Neurology, the Affiliated Hospital of Hangzhou Normal University, Hangzhou 310015, China;

3 Magnetic Resonance Center, Zhongshan Hospital, Medical College of Xiamen University, Xiamen 361004, China;

4 Departments of Respiratory, Zhongshan Hospital, Medical College of Xiamen University, 361004, Xiamen, China.

5 Department of Brain Protection and Plasticity, Institute of Basic Medical Sciences, Beijing 100850, China

[#], authors with equal contributions

Corresponding author:

Jiaxing Zhang, PhD

Department of Physiology and Neurobiology

Medical College of Xiamen University

Xiamen, 361005, China

Tel: +86-0592-2188-421

Email: zhangjiaxing@xmu.edu.cn

Keywords: Brain, chronic obstructive pulmonary disease, grey matter, magnetic resonance images, white matter

Word count: 2961

ABSTRACT

Objectives The irreversible airflow limitation characterized chronic obstructive pulmonary disease (COPD) causes a decrease in oxygen supply to brain. The present study was to investigate brain structural damage in COPD. Design Retrospective case-control study. COPD patients and healthy volunteers were recruited. The two groups were matched in age, gender, and educational background. Setting A hospital and a number of communities: they are all located in southern Fujian province, China. Participants 25 stabled patients and 25 controls were collected from December 2009 to May 2011. Primary and secondary outcome measures Using voxel-based morphometry and tract-based spatial statistics based on MRI to analyze grey matter density and white matter fractional anisotropy (FA), respectively, and a battery of neuropsychological tests were performed. Results COPD patients (vs. controls) showed decreased grey matter density in the limbic and paralimbic structures, including right gyrus rectus, left precentral gyrus, bilateral anterior and middle cingulate gyri, bilateral superior temporal gyri, bilateral anterior insula extending to Rolandic operculum, bilateral thalamus/pulvinars, and left caudate nucleus. COPD patients (vs. controls) had decreased FA values in the bilateral superior corona radiata, bilateral superior and inferior longitudinal fasciculus, bilateral optic radiation, bilateral lingual gyri, left parahippocampal gyrus, and fornix. Lower FA values in these regions were associated with increased radial diffusivity and no changes of longitudinal diffusivity. COPD patients had poor performances in the Mini Mental State Examination, figure memory, and visual reproduction. GM density in some of the above regions in COPD had positive correlations with arterial blood Po_2 while negative correlations with disease duration, and also, had positive correlations with visual tasks. Conclusion We demonstrated that COPD exhibited loss of regional grey matter accompanied by impairment of white matter microstructural integrity, which was associated with disease severity and

may underlie the pathophysiological and psychological changes of COPD.

Funding: This work was supported by National Science Foundation of China (Project No. 31071041; 81171324), Bureau of Science and Technology of Hangzhou (20090833B10), and Health Bureau of Zhejiang Province (2009A168).

Competing interests: None.

Data Sharing: We are pleased to share our original data with all researchers.

SUMMARY

1) Article Focus: Decreased oxygen supply to brain may cause neuronal damage in COPD. However, the damage remains to be largely unknown.

2) Key Messages: We found that COPD extends to the brain, with the loss of regional cortical grey matter accompanied by impairment in the white matter microstructural integrity. > Our findings would be help for clinical therapy of COPD.

3) Strengths and Limitations: Multiple analyses were used based on MR images. The statistic power for FA analysis was weak.

INTRODUCTION

Chronic obstructive pulmonary disease (COPD) continues to be a major cause of morbidity and mortality. It is increasingly recognized that COPD extends beyond the lung.[1] The irreversible airflow limitation characterized COPD usually develops arterial oxygen desaturation, which could subsequently result in a decrease in oxygen transport to the brain. Hypoxia during COPD has been previously proved to induce cerebral perfusion decline[2] and metabolic changes.[3-6] Moreover, systematic inflammation[1] may also cause neuronal damage in the brain of COPD patients. In COPD patients, clinical symptoms such as neuropsychological deficits,[7] depression and anxiety,[1] and physical disability[1] have been well documented. Taken together, all these data suggest the presence of brain structural alteration. However, until now, it remains to be largely uninvestigated.

Voxel-based morphometry (VBM) and Tract-Based Spatial Statistics (TBSS)[8] based on magnetic resonance images (MRI) were adopted to measure grey matter (GM) density and white matter (WM) fibrous microstructure properties in tracts, respectively. VBM is an automatic quantitative volumetric technique over the whole brain using voxel by voxel analysis without prior specification of regions of

interest for analysis and it does not rely on arbitrarily predefined structures. Recently, the preprocessing steps of VBM have been improved with the Diffeomorphic Anatomical Registration Through Exponentiated Lie algebra (DARTEL) registration method,[9] which can achieve more accurate inter-subject registration of brain images. TBSS is a recently introduced method, which uses diffusion tensor MR imaging (DTI) to measure differences in fractional anisotropy (FA) between groups. TBSS increases the sensitivity and the interpretability of the results compared with voxel-based approaches based purely on non-linear registration.[8] Moreover, diffusion tensor eigenvalues (longitudinal diffusivity [the magnitude of diffusion along the principal diffusion direction, λ1] and radial diffusivity [the magnitude of diffusion in the two orthogonal directions perpendicular to the principal diffusion direction, λ23]) were also included in the analysis since they can help interpret FA changes in WM tracts by providing information regarding likely alterations in the proportion of longitudinally vs. obliquely aligned myelinated fibers. The VBM and TBSS methods have been extensively applied in clinical researches, including the evaluation of morphological characteristics of high-altitude residents in our previous study.[10]

Dyspnea is the most common complaint and most disabling symptom in patients with COPD. Functional MRI studies on breathlessness, air hunger, and inspiratory loaded breathing have revealed that a large number of brain regions, including the frontal cortex, parietal cortex, temporal cortex, limbic cortex, cerebellar cortex, and brainstem, were activated by dyspnea.[11] These dyspnea-activated brain regions have been shown to be impaired in congenital central hypoventilation syndrome patients,[12] in obstructive sleep apnea patients,[13] and in high-altitude residents.[10] We therefore hypothesized that COPD patients would have similar cerebral impairment.

METHODS

Subjects

Twenty-five patients were collected from December 2009 to May 2011. All patients had undergone a period 30 to 45 days of in-hospital rehabilitation following an acute exacerbation of COPD. At the time of data collection, patients were in stable condition. Among these patients, 12 discharged patients were recruited during their rest at home and 13 patients were recruited when they were awaiting discharge from hospital. Patients were diagnosed at stage I (4%), stage II (32%), stage III (28%) and stage IV (36%) in Zhongshan hospital (Xiamen, China) according to the diagnostic criteria of Global Initiative for Chronic Obstructive Lung Disease (GOLD).[14] Twenty-five healthy volunteers, with comparable age, gender, and educational background, comprised the control group. All the subjects were free from a known history of cerebrovascular accident, heart failure, neurological disorders, OSA, coronary artery disease, diabetes, or other diseases known to affect cognition. Patients were provided with therapy including inhaled ipratropium bromide, bricanyl, ventoline, and budesonide. Demographic characteristics of the patients and healthy volunteers were listed in Table 1. Procedures were fully explained and all subjects were provided written informed consent before participating in the study. The experimental protocol was approved by the Research Ethics Review Board of Xiamen University.

Physiological and neuropsychological tests

Physiological and neuropsychological tests and activities of daily living (ADL) (score range 14-56)[15] were conducted one day before MRI scan. Physiological tests include pulse rate and arterial blood pressure measures, arterial blood gas analysis, and pulmonary function measure. Blood samples were taken in the morning at 0700-0730 h. The neuropsychological tests include: (i) the Chinese version of

the Mini Mental State Examination (MMSE) measured the general cognitive function. (ii) the visual reproduction test, figure memory test, and digital span forward and backward tasks, which taken from the Chinese revised version of Wechsler Memory Scale, were used to measure visual construction ability, visuospatial memory, and short-term working memory, respectively [16]. All data were analyzed using SPSS 19.0 (Chicago, IL, USA). Independent t test measures between-group differences. Statistical significance was set at $p < 0.05$.

MRI data acquisition

Images were acquired on a Siemens Trio Tim 3.0T (Erlangen, Germany) at MRI Research Center (Zhongshan Hospital, Xiamen, China). A 3D structural MRI was acquired from each subject using a T1-weighted MPRAGE sequence (TR/TE = 1900 ms/2.48 ms, FOV = 25 × 25 cm^2, NEX = 1, matrix = 512 × 256, slice thickness = 1.0 mm). Conventional 2D T1 and T2 images were also acquired and examined for any incidental findings. A DTI pulse sequence with single shot diffusion-weighted echo planar imaging (TR/TE = 3600/95 ms, FOV=24 × 24 cm^2, NEX = 2, matrix = 128 × 128, slice thickness = 4.5 mm) was applied sequentially in 30 non-collinear directions (b-value = 1000s/ mm^2) with one scan without diffusion weighting (b = 0s/mm^2). The following data analyses were conducted by two researchers who were blind to the status of subjects.

VBM analysis of 3D T1 images

The 3D T1 images were used for GM analysis using VBM8 toolbox implemented in SPM8 (Wellcome Department of Imaging Neuroscience, University College London, London, UK). The following processing steps were carried out: (i) the images were inspected and set at the anterior commissure.

Each reorientated image was segmented into GM, WM and CSF in native space and procrustes aligned GM images were generated by a rigid transformation. (ii) the DARTEL was used to create study-specific template by the aligned images from all the patients and controls to improve inter-subject registration of structural images.[9] The procedure implicated in six iterations, which began with the averaging of aligned data to generate an original template. Then, the first iteration of the registration was done on each subject and a new template was created. After this, the second iteration began. When six iterations were finished, the template was generated, which was the average of the DARTEL registered data. During iterations, all images were warped to the template yielding a series of flow fields that parameterized deformations. (iii) the normalized images were transformed into MNI space. These GM images were then smoothed using a Gaussian kernel of 8 mm full-width at half-maximum. Independent t-tests were performed to examine between-group differences. The statistical parametric map was generated with threshold at $t > 3.7734$, $p < 0.01$ (FDR correction with gender, age, education, and total intracranial volume as covariates).

To analyze the correlation of GM image value with cognitive or physiological measurement, the following steps were first done: (1) Regions-of-interests were created for clusters showing differences between groups; (2) using these Regions-of-interests masks, the GM values were extracted from each individual's normalized and smoothed GM maps. Then the correlations were analyzed using SPSS. Statistical significance was set at $p < 0.05$.

TBSS analysis of DTI

DCM2MII was used to convert diffusion tensor images from the proprietary scanner format to the NIFTI format. Then images were processed using FSL 4.1.5 software package

(http://www.fmrib.ox.ac.uk/fsl/). Images were realigned to the b-value (b0) image by affine transformations using FMRIB's diffusion toolbox (FDT) [17] to minimize distortions and reduce head motion artifacts. In order to remove non-brain tissue components and background noise, brain mask was created from the first b0 image, and then applied in the DTI to extract brain voxels using Brain Extraction Tool (BET). After these processes, using DTIFit within the FDT, images were calculated to get the FA, λ1, and λ23 maps. The whole brain voxel-wise statistic analysis of FA images was performed using TBSS in FSL.[7] TBSS processing includes the following steps: (i) align the FA images of all subjects to a template which was arbitrarily selected from those FA images by nonlinear registrations; (ii) transform all the aligned FA images into 1×1×1 mm^3 MNI152 space by affine registrations to remove the effect of cross-subject spatial variability that remains after the non-linear registration; (iii) create the mean FA image and filter to retain only the center of the WM tracts, with the threshold FA ≥ 0.20, and successfully exclude voxels, which consisted of GM or CSF in the majority of subjects, so as to create the mean FA skeleton. (iv) project individual subjects' FAs onto mean FA skeleton. (v) following these steps, data were fed into voxel-wise cross-subject statistical analyses. In all cases, the null distribution was built up over 5000 permutations, with significance analyzed using independent t-tests at $p < 0.05$ levels, uncorrected for multiple comparisons. We determined the anatomic localization of each cluster by means of the FSL atlas tool, which incorporates several anatomic templates, including the Harvard-Oxford Cortical Structural Atlas, Harvard-Oxford Subcortical Structural Atlas, Talairach Daemon Labels, and MNI Structural Atlas.

Within the cluster of changed FA, mean λ1 and λ23 values were extracted from each individual's λ1 and λ23 maps. Values were analyzed using SPSS. ANOVA statistic to identify the group differences for these distinct brain locations. Statistical significance was set at $p < 0.05$.

RESULTS

Physiological and behavioral findings (Table 2)

Compared with the controls, Independent t test showed that COPD patients had significant decreases in arterial blood Sao_2 and Po_2, and increases in arterial blood Pco_2 and heart rate. COPD patients had significant lower one second over forced vital capacity (FVC), forced expiratory volume (FEV), and FEV1/FVC values and higher respiratory rate. COPD patients had significant lower scores in ADL, MMSE test, visual reproduction, and figure memory.

GM density

No subject from either group showed visible abnormalities on T1-weighted structural images. VBM analysis showed that COPD patients had decreased GM densities compared with healthy controls in the right gyrus rectus, left precentral gyrus, bilateral anterior and middle cingulate gyri, bilateral superior temporal gyri, bilateral anterior insula extending to Rolandic operculum (base of the pre- and post-central gyri), bilateral thalamus/pulvinars, and left caudate nucleus (cluster size > 100 voxels) (Fig. 1-4, Table 3).

FA, longitudinal diffusivity, and radial diffusivity in relation to COPD

Whole brain voxel-wise statistic analysis showed COPD patients had significantly lower FA in a broad range of brain regions compared with controls (Fig. 5, Table 4). The significantly affected regions (clusters size > 40 voxels) included the superior corona radiata (corresponding to bilateral precuneus and bilateral superior parietal lobules), superior longitudinal fasciculus (bilateral supramarginal gyri),

inferior longitudinal fasciculus (left superior temporal gyrus, right middle temporal gyrus, and fusiform gyrus), bilateral optic radiation, bilateral lingual gyri, left parahippocampal gyrus, and fornix.

Lower FA values in these regions were associated with increased radial diffusivity and no changes of longitudinal diffusivity in COPD patients vs. controls (Table 4).

Correlations between MRI measurement and disease severity

The correlations were listed in Table 5. In COPD patients, partial correlation (controlling for disease duration, FEV1/FVC, age, education, and gender) revealed GM density in the bilateral anterior cingulate cortex, left superior temporal cortex, bilateral insula/superior temporal/Rolandic Operulum, bilateral thalamus/Pulvinar, and left caudate nucleus had positive correlations with arterial blood Po_2. Partial correlation (controlling for Po_2, FEV1/FVC, age, education, and gender) revealed GM density in the bilateral anterior cingulate cortex, right insula/superior temporal/Rolandic Operulum, and right thalamus/Pulvinar had negative correlations with disease duration. Partial correlation (controlling for age, education, and gender) analysis showed that the GM density in the left superior temporal lobes and left insula/superior temporal/Rolandic Operculum in COPD patients was significantly correlated with figure memory score and the GM density in left precentral gyrus and left thalamus/Pulvinar in COPD patients was significantly correlated with visual reproduction.

DISCUSSION

Our present study revealed that COPD patients had decreased regional GM density confined to the limbic and paralimbic structures. GM density in impaired regions in COPD patients had significant positive correlation with arterial blood Po_2 and negative correlation with disease duration. The

decreased WM FA value with increased radial diffusivity value was detected mainly in the visual cortex of occipital lobe, the posterior parietal lobe as well as the temporal lobe. Decreased FA was associated with compromised myelin structure, changes in axonal morphologic structure, and altered interaxonal spacing of fiber bundles.[18] Radial diffusivity measures motion of water molecules perpendicular to fibers and increase of radial diffusivity is interpreted as abnormalities in myelinated membranes.[19] Consequently, decreased FA and increased radial diffusivity in COPD indicated the impairment of WM microstructural integrity.

Previously, Borson et al.[6] only measured the volume of hippocampus in COPD patients using region-of-interest analysis and did not find significant change as our measured using VBM. The impaired brain regions in COPD have also been found in other chronic hypoxic diseases. For example, decrease of GM volume/concentration in the gyrus rectus, precentral gyrus, anterior cingulate cortex, multiple sites within the temporal lobes, insular cortex, thalamus, and caudate nucleus were detected in patients with obstructive sleep apnea.[13] Impairments of WM microstructure in the temporal lobe, parietal lobe, fornix, and corona radiata were found in patients with congenital central hypoventilation syndrome.[12] In our previous study, the decrease of GM volume in the anterior insula, anterior cingulate cortex, and precentral cortex were found on high-altitude residents.[10]

GM density in impaired regions in COPD patients had strongly positive correlation with the arterial blood Po_2, which suggested the impairment in GM may result from low blood oxygen. Moreover, the GM density in some impaired regions showed negative correlations with disease duration, suggesting the more GMs were lost with low oxygen persists. It is already known that hypoxia can induce metabolic decreases[3-5] and cerebral perfusion decline[2] in COPD. In addition, COPD patients often suffer from systemic inflammation, which can exacerbate neuronal injury.[1] A greater proportion of

regions showing GM loss located in limbic/paralimbic cortex in COPD patients may be due to that those phylogenetically older regions of the brain showed sharper vascular responses to hypoxia than evolutionary younger regions.[20]

Morphological impairments in anterior insula and anterior cingulate cortex could play a role in respiratory and cardiovascular responses to dyspnea, because a larger cortical network including these regions underlie the perception of dyspnea[11] and play an important role in regulating the cardiovascular system.[21] The impaired GM in posterior thalamus may clarify the enhanced breathing movements in COPD patients, because it has been proved to be implicated in suppressing the ventilatory response to hypoxia.[22] Hippocampus has been proved to control arterial pressure and heart rate.[23] Therefore, decreased GM or impaired connect fibers, such as fornix, in these areas may elucidate cardiovascular disturbances in COPD patients.[1]

In the present study, COPD patients had poorer performance in MMSE, visuospatial memory, and visual construction task. These results were consistent with that found in previous studies in COPD patients.[7] In line with the present findings in COPD, we previously found that long-time living at mild high-altitude hypoxic environment impaired cognitive performances only confined to visual reproduction and short-time complex figure memory.[24] In our present study, the decreases of GM density in frontal precentral cortex, insula/superior temporal cortex/Rolandic Operculum, and thalamus/pulvinar may be responsible for the deficit in visual-related tasks since the GM density in these areas showed a significantly positive correlation with figure memory or visual reproduction score. The following previous data may support our findings: (i) Recent research has identified the inferior frontal cortex served as a source of top-down modulation underlying attention to visual features.[25] (ii) Studies on patients using fMRI and PET demonstrated Rolandic operculum as one of the visual

structures.[26] (iii) The pulvinar region of the thalamus is known to project to posterior parietal lobe and inferior temporal lobe. The pulvinar has been implicated in various visual functions in lesion studies.[27] Declines in memory and executive function make contributions to declines in ADL.[28] Visual construction task reflects executive function. Therefore, the decreases of GM density in the above regions that relate to visual construction may also be responsible for ADL deficits.

Our present study found the impairments of WM limited to the pathways of visual processing, including optic radiation, posterior parietal lobe (superior parietal lobule, supramarginal gyrus, and precuneus), and the inferior temporal fusiform and lingual gyri. Visual information enters the primary visual cortex via optic radiation to the visual cortex. Cortical areas along the posterior parietal 'dorsal stream' are primarily concerned with spatial localization and directing attention, while cortical areas along the inferior temporal 'ventral stream' are mainly concerned with the recognition and identification of visual stimuli.[29] COPD also showed impaired WM in middle temporal gyrus. Middle temporal cortex is important for the long-term buildup of perceptual memory for ambiguous motion stimuli.[30] Based on the above data, our findings in WM may also clarify the mechanisms underling the deficit in visual-related tasks. In addition, impaired WM in input and output fibers of hippocampus (fornix) may be related to the deficit in MMSE. Previous study on patients with Alzheimer's disease found the volumes of hippocampus were significantly reduced and the volumes of the left hippocampus correlated significantly with the MMSE score.[31] The limitation of our study is the weak statistical power of FA value analysis, because the results obtained in the TBSS analysis could not survive multiple comparison correction.

Conclusions

In summary, we first demonstrated that COPD extended beyond the lung to the brain, with the decrease of regional GM density accompanied by impairment in the WM microstructural integrity. Our findings suggest significant participation of these structures in responding to hypoxic challenges, which include cardiovascular and air-hunger components. The brain structural changes may also underlie the psychological and mood changes of COPD.

Authors' contributions

Haiyan Zhang: contributed to the study design, take responsibility for the integrity of the data, the accuracy of the data analysis.

Xiaochuan Wang: contributed to the study design, collection, analysis, and interpretation of data, and critical review.

Jianzhong Lin: contributed to the collection, analysis, and interpretation of data.

Yingchun Sun: contributed to the collection, analysis, and interpretation of data.

Yongxia Huang: contributed to the collection, analysis, and interpretation of data.

Tianhe Yang: contributed to the collection, analysis, and interpretation of data.

Shili Zheng: contributed to the collection, analysis, and interpretation of data.

Ming Fan: contributed to the study design, drafting, critical review, and final approval of the manuscript.

Jiaxing Zhang: contributed to conception and design, interpretation of data, drafting the article, and final approval of the manuscript.

Table 1 Demographic characteristics of the patients with COPD and healthy volunteers

	COPD patients	Controls	p
Number of subjects	25	25	
Gender (female) (%)	16	16	
Age (years) (mean ± SD)	69.2 ± 8.1 (58 - 84)	67.96 ± 8.0 (57 - 86)	0.59
Education (years) (mean ± SD)	6.7 ± 3.9	7.5 ± 5.0	0.53
Family history of COPD (%)	4	-	
Disease duration (years)	7.0 ± 5.7	-	
Actual smokers (%)	44	40	0.86

Table 2 Physiological and psychological characteristics

	COPD patients	Controls	*P*
BMI (kg/m^2)	20.8 ± 3.9	22.6 ± 2.6	0.081
ADL	20.12 ± 6.5	14.6 ± 1.52	<0.001
Heart rate	92.4 ± 16.2	70.9 ± 8.94	<0.001
Blood pressure (mmHg)			
systolic pressure	136.1±19.1	136.5 ± 18.0	0.940
diastolic pressure	81.8 ± 10.7	77.5 ± 14.5	0.307
Hematological measurements			
Sao_2 (%)	94.0 ± 4.2	97.0 ± 1.3	0.003
Po_2 (mmHg)	79.9 ± 23.3	98.5 ± 11.3	0.006
Pco_2 (mmHg)	48.1 ± 6.0	39.8 ± 3.0	<0.001
pH	7.37 ± 0.06	7.36 ± 0.01	0.731
Pulmonary Function testing			
Respiratory rate (breaths/min)	23.5 ± 6.0	16.9 ± 5.5	0.003
FVC (% predicted)	66.6 ± 17.2	96.1 ± 14.7	<0.001
FEV1 (% predicted)	43.4 ± 16.4	97.5 ± 16.9	<0.001
FEV1/ FVC (%)	50.31 ± 10.7	80.0 ± 8.32	<0.001

Cognitive tests			
MMSE	23.3 ± 3.4	25.8 ± 2.1	0.021
Digit Span			
Forward task	7.0 ± 1.6	7.7 ± 1.4	0.125
Backward task	4.1 ± 1.9	4.3 ± 1.5	0.612
Visual reproduction	8.2 ± 3.4	10.3 ± 3.0	0.031
Figure memory	10.5 ± 3.0	12.4 ± 1.9	0.010

ADL, activities of daily living; BMI, body mass index; FEV1, forced expired volume in one second; FVC, forced vital capacity; MMSE, Mini Mental State Examination. Data are mean ± SD.

Table 3 Regional information of decreased grey matter density (cluster size > 100 voxels) in COPD patients compared with healthy controls

Area	**Volume**	**Brodmann**	**MNI coordinate**			**t-score**
	(mm^3)	**areas**	**x**	**y**	**z**	**(peak)**
Rectus_R	118	11	9	39	-20	4.31
Precentral_L	100	6	-51	-5	33	4.95
Cingulum_Ant_R	485	32	8	38	17	5.88
Cingulum_Ant_L	212	32	-8	38	18	4.49
Cingulum_Mid_R	157	24	6	-9	42	4.87
Cingulum_Mid_L	136	24	-6	-9	41	4.91
Temporal_Sup_ L	280	22/42	-60	-33	3	4.99
Temporal_Sup/ Rolandic_Oper _L	837	22	-57	-14	10	4.91
Insula/Temporal_Sup/ Rolandic_Oper _R	2821	13/22/47	44	11	-5	5.15
Insula/Temporal_Sup/ Rolandic_Oper _L	1551	13/22/47	-33	12	-15	4.48
Thalamus/Pulvinar_L	1270		-12	-30	3	6.46
Thalamus/Pulvinar_R	2210		12	-26	8	5.29
Caudate_L	212		-9	14	14	4.19

Table 4 Main regions showing FA, λ1, λ23 values in COPD patients compared with healthy controls

MNI (peak)			Voxels	White matter	Corresponding cortical area	FA value		λ1 (×10^3 mm^2/s)		λ23 (×10^3 mm^2/s)	
x	y	z	(mm^3)	tract		COPD	Control	COPD	Control	COPD	Control
1	10	16	240	Fornix	Fornix	0.248(0.067)	0.289(0.073)	2.586(0.314)	2.406(0.0321)	1.809(0.295)	1.577(0.262)*
-26	-69	1	191	Lingual gyrus	Left lingual gyrus	0.259(0.042)	0.283(0.046)	1.450(0.240)	1.370(0.224)	0.992(0.185)	0.896(0.168)*
27	-53	3	147	Lingual gyrus	Right lingual gyrus	0.265(0.065)	0.290(0.056)	1.381(0.239)	1.346(0.227)	0.955(0.242)	0.891(0.215)*
-23	-19	-24	77	Parahippocampus	Left parahippocampus	0.268(0.042)	0.319(0.046)	1.234(0.057)	1.189(0.052)	0.869(0.148)	0.771(0.125)*
38	-24	-24	77	fusiform gyrus	Right fusiform gyrus	0.231(0.037)	0.248(0.046)	1.053(0.063)	1.094(0.073)	0.774(0.030)	0.723(0.032)*
-10	-91	17	204	Optic radiation	Left occipital cortex	0.234(0.043)	0.277(0.041)	1.037(0.038)	1.020(0.031)	0.752(0.063)	0.693(0.051)*
25	-86	-5	200	Optic radiation	Right occipital cortex	0.369(0.099)	0.409(0.122)	1.171(0.014)	1.177(0.171)	0.649(0.057)	0.601(0.071)*
-9	-72	45	94	SCR	Left precuneus	0.283(0.053)	0.317(0.056)	1.099(0.032)	1.069(0.041)	0.726(0.075)	0.665(0.065)*
9	-66	37	57	SCR	Right precuneus	0.251(0.030)	0.280(0.044)	1.044(0.032)	1.018(0.023)	0.868(0.073)	0.731(0.084)*
-15	-51	62	57	SCR	Left superior parietal lobule	0.267(0.043)	0.294(0.043)	1.130(0.051)	1.082(0.025)	0.724(0.039)	0.671(0.045)*
16	-45	64	66	SCR	Right superior parietal lobule	0.251(0.043)	0.294(0.051)	1.176(0.117)	1.107(0.094)	0.805(0.056)	0.762(0.056)*
-45	-53	31	44	SLF	Left supramarginal gyrus	0.221(0.027)	0.239(0.026)	1.088(0.020)	1.076(0.040)	0.935(0.090)	0.873(0.071)*
37	-68	21	63	SLF	Right supramarginal gyrus	0.220(0.025)	0.237(0.025)	1.116(0.039)	1.090(0.052)	0.773(0.076)	0.715(0.007)*
-48	0	-16	43	ILF	Left superior temporal gyrus	0.244(0.013)	0.270(0.021)	1.060(0.030)	0.984(0.015)	0.758(0.025)	0.714(0.037)*
53	-46	-6	41	ILF	Right middle temporal gyrus	0.206(0.016)	0.241(0.024)	1.025(0.016)	1.006(0.021)	1.605(0.167)	1.340(0.139)*

ILF, inferior longitudinal fasciculus; SCR, superior corona radiata; SLF, superior longitudinal fasciculus. Data are presented as means (SD). *p<0.05.

Table 5 Correlations of grey matter density in impaired regions with Po_2, disease duration, and cognitive performances in patients with COPD

Area	Po_2 (patients)	Disease duration (patients)	Cognitive performances (patients + controls)	
			figure memory	visual reproduction
Precentral_L				r=0.306, p=0.028
2Cingulum_Ant_R	r=0.530, p=0.021	r=-0.471, p=0.038		
1Cingulum_Ant_L	r=0.744, p=0.001	r=-0.476, p=0.036		
Cingulum_Mid_R				
Cingulum_Mid_L				
11Temporal_Sup_L	r=0.713, p=0.001		r=0.511, p=0.001	
Temporal_Sup/ Rolandic_Oper _L				
6Insula/Temporal_Sup/ Rolandic_Oper _R	r=0.615, p=0.007			
7Insula/Temporal_Sup/Rolandic_Oper _L	r=0.656, p=0.004		r=0.498, p=0.001	
9Thalamus/Pulvinar_L	r=0.487, p =0.033	r=-0.474, p=0.037		r=0.284, p =0.044
8Thalamus/Pulvinar_R	r=0.502, p =0.028	r=-0.517, p=0.024		
5Caudate_L	r=0.550, p=0.017			

REFERENCES

1. Barnes PJ. Chronic obstructive pulmonary disease: effects beyond the lungs. *PLoS Med* 2010; 7:e1000220.

2. Ortapamuk H, Naldoken S. Brain perfusion abnormalities in chronic obstructive pulmonary disease: comparison with cognitive impairment. *Ann Nucl Med* 2006; 20:99-106.

3. Shim TS, Lee JH, Kim SY, *et al*. Cerebral metabolic abnormalities in COPD patients detected by localized proton magnetic resonance spectroscopy. *Chest* 2001; 120:1506-13.

4. Sicard KM, Duong TQ. Effects of hypoxia, hyperoxia, and hypercapnia on baseline and stimulus-evoked BOLD, CBF, and CMRO2 in spontaneously breathing animals. *Neuroimage* 2005; 25:850-8.

5. Sinha S, Kumar V, Jagannathan NR, *et al*. Proton magnetic resonance spectroscopy of brain to study the cerebral metabolic abnormalities in COPD patients: a case control study in north India. *Indian J Chest Dis Allied Sci* 2009; 51:15-9.

6. Borson S, Scanlan JM, Friedman S, *et al*. Modeling the impact of COPD on the brain. *International Journal of Chronic Obstructive Pulmonary Disease* 2008; 3: 429-34.

7. Dodd JW, Getov SV, Jones PW. Cognitive function in COPD. *Eur Respir J* 2010; 35:913-22.

8. Smith SM, Jenkinson M, Johansen-Berg H, *et al*. Tract-based spatial statistics: voxelwise analysis of multi-subject diffusion data. *Neuroimage* 2006; 31:1487-505.

9. Ashburner J. A fast diffeomorphic image registration algorithm. *Neuroimage* 2007; 38:95-113.

10. Zhang J, Yan X, Shi J, *et al*. Structural modifications of the brain in acclimatization to high-altitude. *PLoS One* 2010; 5:e11449.

11. von Leupoldt A, Dahme B. Cortical substrates for the perception of dyspnea. *Chest* 2005; 128:345-54.

12. Kumar R, Macey PM, Woo MA, *et al*. Diffusion tensor imaging demonstrates brainstem and cerebellar abnormalities in congenital central hypoventilation syndrome. *Pediatr Res* 2008; 64:275-80.

13. Joo EY, Tae WS, Lee MJ, *et al*. Reduced brain gray matter concentration in patients with obstructive sleep apnea syndrome. *Sleep* 2010; 33:235-41.

14. Pauwels RA, Buist AS, Calverley PM, *et al*. Global strategy for the diagnosis, management, and prevention of chronic obstructive pulmonary disease. NHLBI/WHO Global Initiative for Chronic Obstructive Lung Disease (GOLD) Workshop summary. *Am J Respir Crit Care Med* 2001; 163:1256-76.

15. Lawton MP, Brody EM. Assessment of older people: self-maintaining and instrumental activities of daily living. *Gerontologist* 1969; 9:179-86.

16. Gong YX. Manual for the Wechsler Memory Scale-Revised. Hunan Medical University. Changsha,

Hunan, China. 1989.

17. Jenkinson M, Smith S. A global optimisation method for robust affine registration of brain images. *Med Image Anal* 2001; 5:143-56.

18. Beaulieu C. The basis of anisotropic water diffusion in the nervous system - a technical review. *NMR Biomed* 2002; 15:435-55.

19. Song SK, Sun SW, Ramsbottom MJ, *et al*. Dysmyelination revealed through MRI as increased radial (but unchanged axial) diffusion of water. *Neuroimage* 2002; 17:1429-36.

20. Binks AP, Cunningham VJ, Adams L, *et al*. Gray matter blood flow change is unevenly distributed during moderate isocapnic hypoxia in humans. *J Appl Physiol* 2008; 104:212-7.

21. Nagai M, Hoshide S, Kario K. The insular cortex and cardiovascular system: a new insight into the brain-heart axis. *J Am Soc Hypertens* 2010; 4:174-82.

22. Teppema LJ, Dahan A. The ventilatory response to hypoxia in mammals: mechanisms, measurement, and analysis. *Physiol Rev* 2010; 90:675-754.

23. Macefield VG, Gandevia SC, Henderson LA. Neural sites involved in the sustained increase in muscle sympathetic nerve activity induced by inspiratory capacity apnea: a fMRI study. *J Appl Physiol* 2006; 100:266-73.

24. Zhang J, Liu H, Yan X, *et al*. Minimal effects on human memory following long-term living at moderate altitude. *High Alt Med Biol* 2011; 12:37-43.

25. Zanto TP, Rubens MT, Bollinger J, *et al*. Top-down modulation of visual feature processing: the role of the inferior frontal junction. *Neuroimage* 2010; 53:736-45.

26. Fried I, Nenov VI, Ojemann SG, *et al*. Functional MR and PET imaging of rolandic and visual cortices for neurosurgical planning. *J Neurosurg* 1995; 83:854-61.

27. Arend I, Machado L, Ward R, *et al*. The role of the human pulvinar in visual attention and action: evidence from temporal-order judgment, saccade decision, and antisaccade tasks. *Prog Brain Res* 2008; 171:475-83.

28. Tomaszewski Farias S, Cahn-Weiner DA, Harvey DJ, *et al*. Longitudinal changes in memory and executive functioning are associated with longitudinal change in instrumental activities of daily living in older adults. *Clin Neuropsychol* 2009; 23:446-61.

29. Itti L, Koch C. Computational modelling of visual attention. *Nat Rev Neurosci* 2001; 2:194-203

30. Brascamp JW, Kanai R, Walsh V, *et al*. Human middle temporal cortex, perceptual bias, and perceptual memory for ambiguous three-dimensional motion. *J Neurosci* 2010; 30:760-6.

31. Laakso MP, Soininen H, Partanen K, *et al*. Volumes of hippocampus, amygdala and frontal lobes in the MRI-based diagnosis of early Alzheimer's disease: correlation with memory functions. *J Neural Transm Park Dis Dement Sect* 1995; 9:73-86.

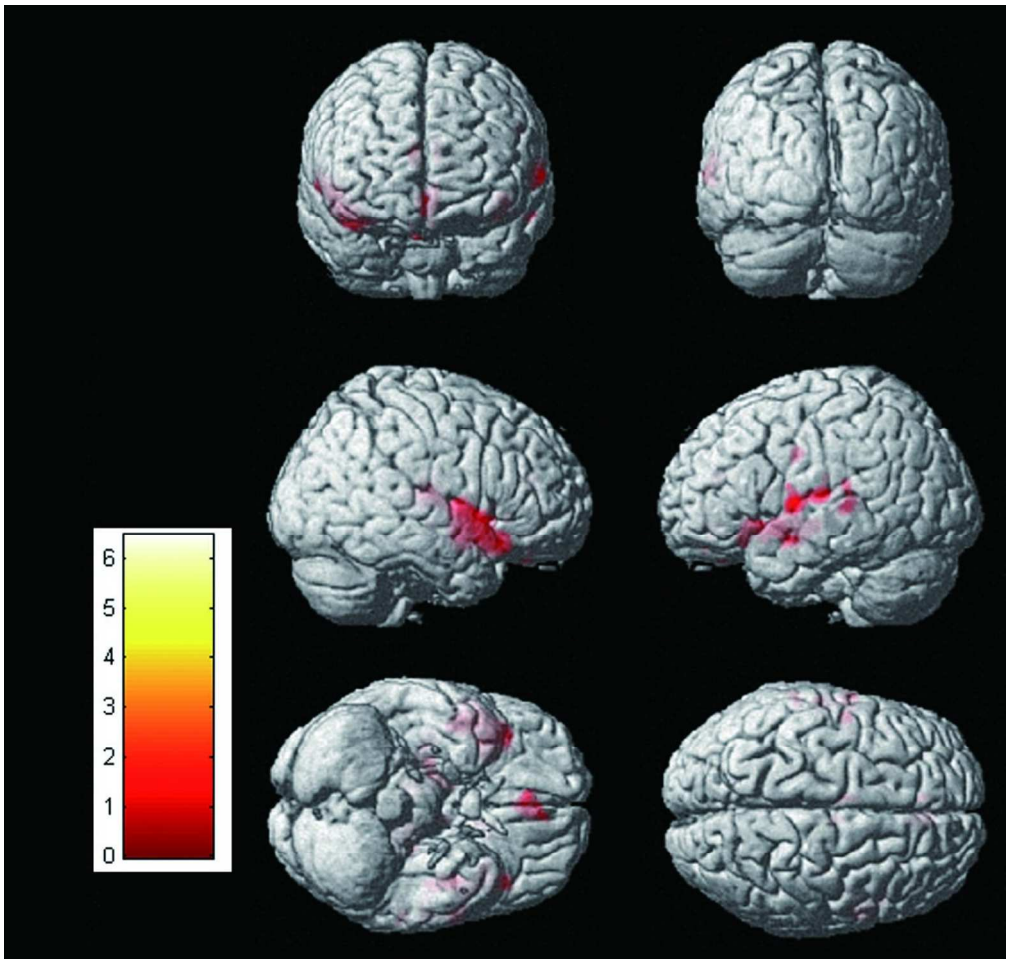

Figure 1 A statistical parametric map for grey matter density reduced in COPD patients vs. healthy controls (pFDR_corrected< 0.01) overlaid on the MNI template.

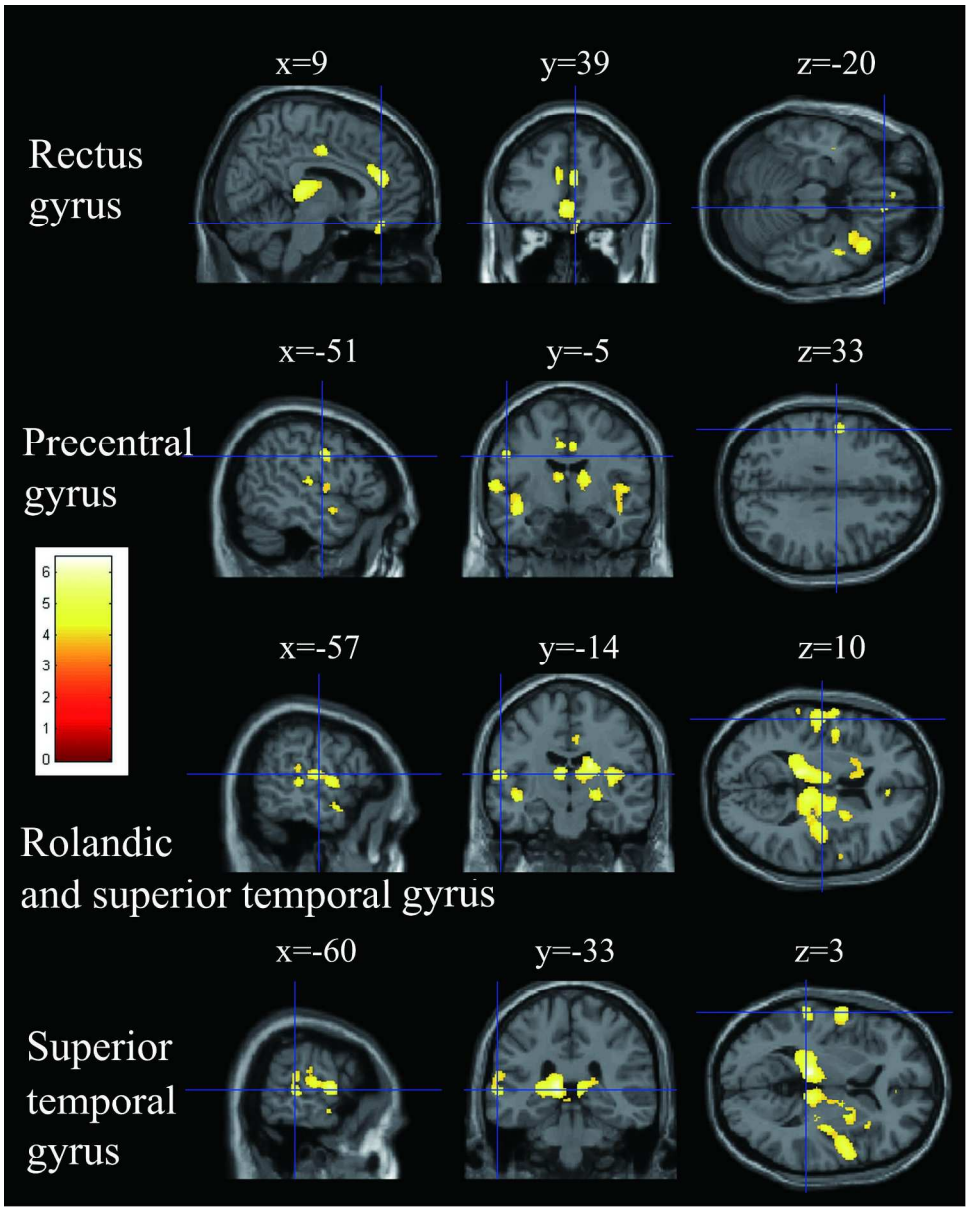

Figure 2 Grey matter density decrease in COPD patients vs. healthy controls. Three-dimensional slices depicting regions showing reduced grey matter in the right gyrus rectus, left precentral gyrus, left Rolandic operculum and superior temporal gyrus overlaid on a T1-weighted MRI anatomical image in the MNI template.

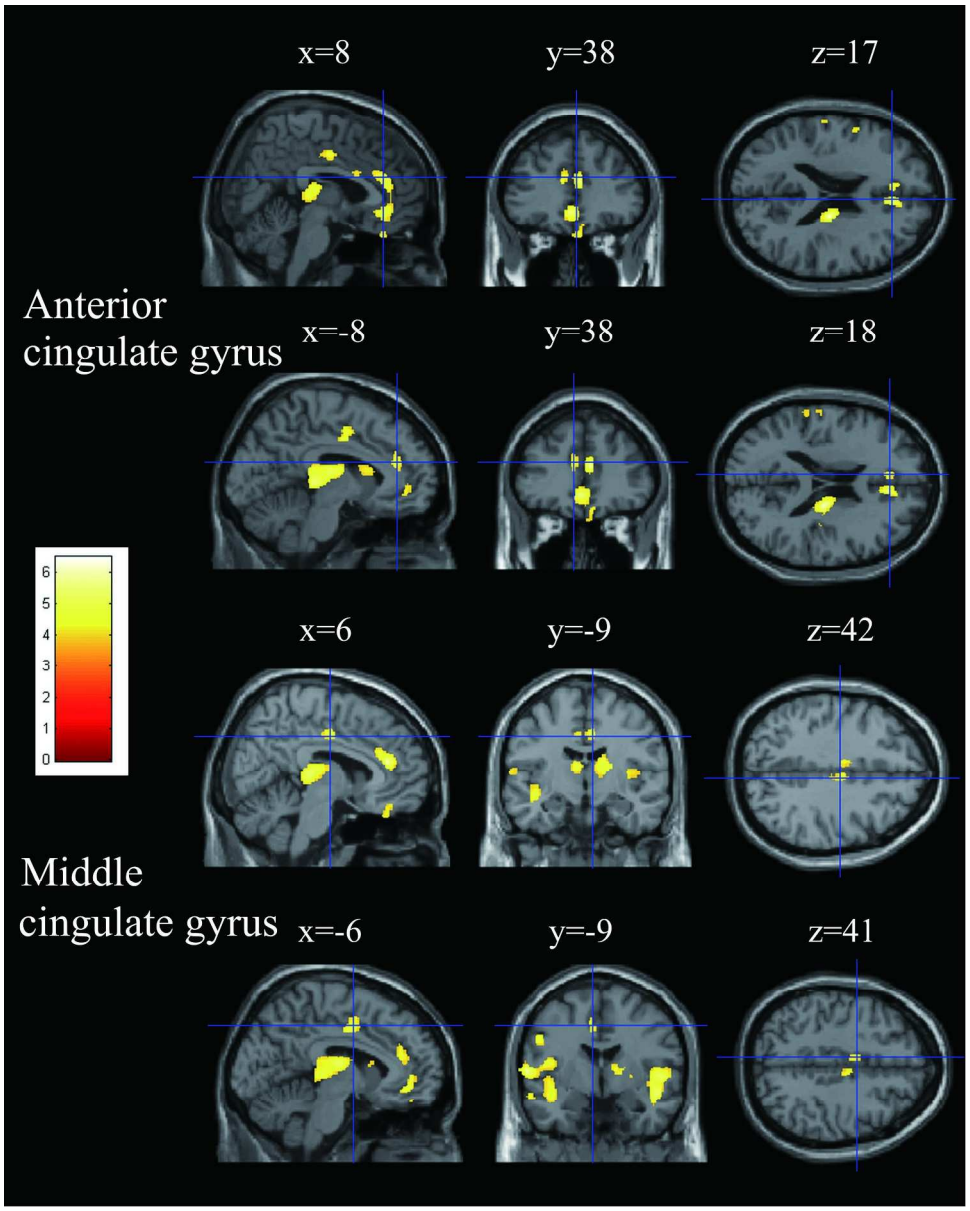

Figure 3 Grey matter density decrease in COPD patients vs. healthy controls. Three-dimensional slices depicting regions showing reduced grey matter in the bilateral anterior and middle cingulate gyri overlaid on a T1-weighted MRI anatomical image in the MNI template.

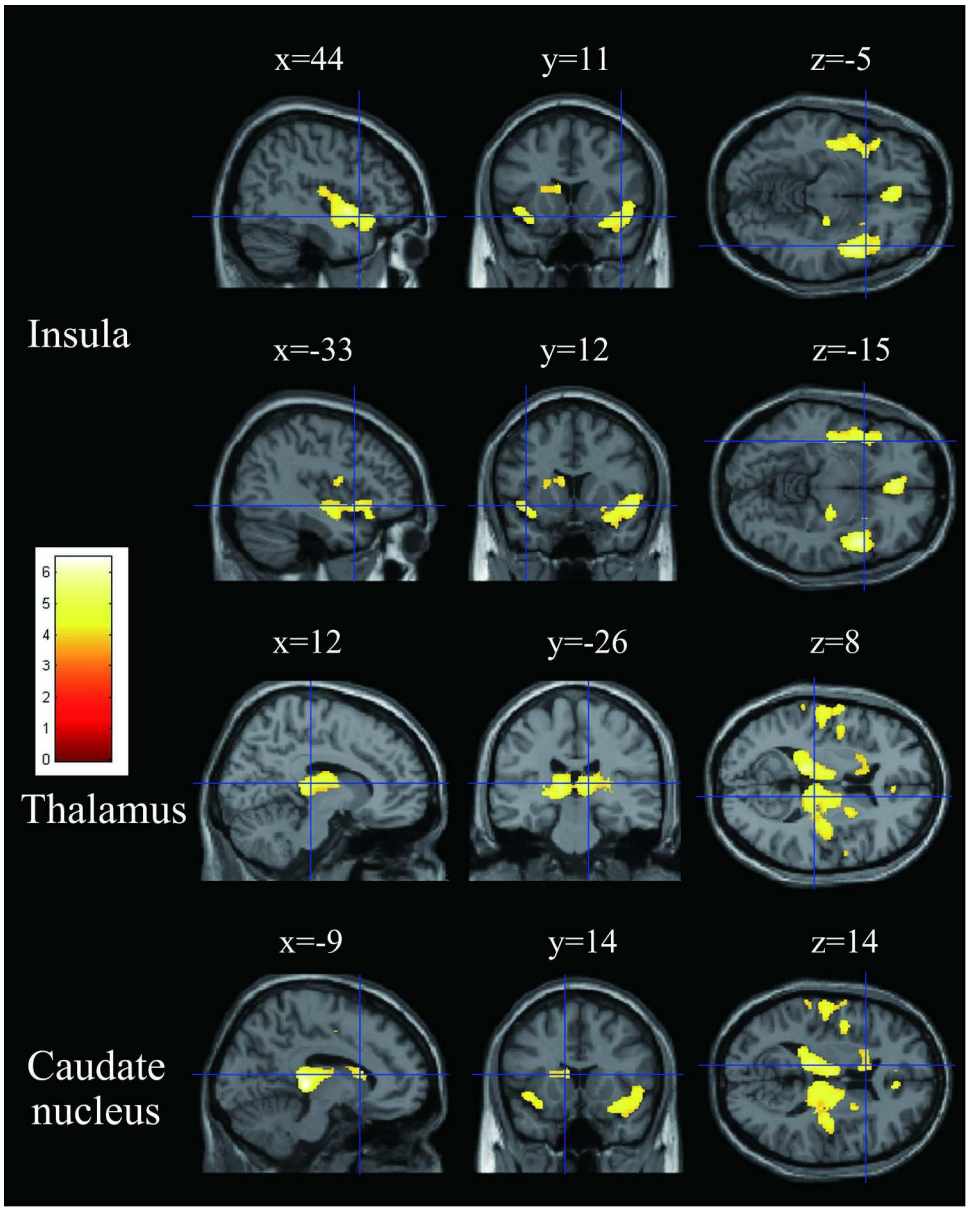

Figure 4 Grey matter density decrease in COPD patients vs. healthy controls. Three-dimensional slices depicting regions showing reduced grey matter in the bilateral insula, bilateral thalamus, and left caudate nucleus overlaid on a T1-weighted MRI anatomical image in the MNI template.

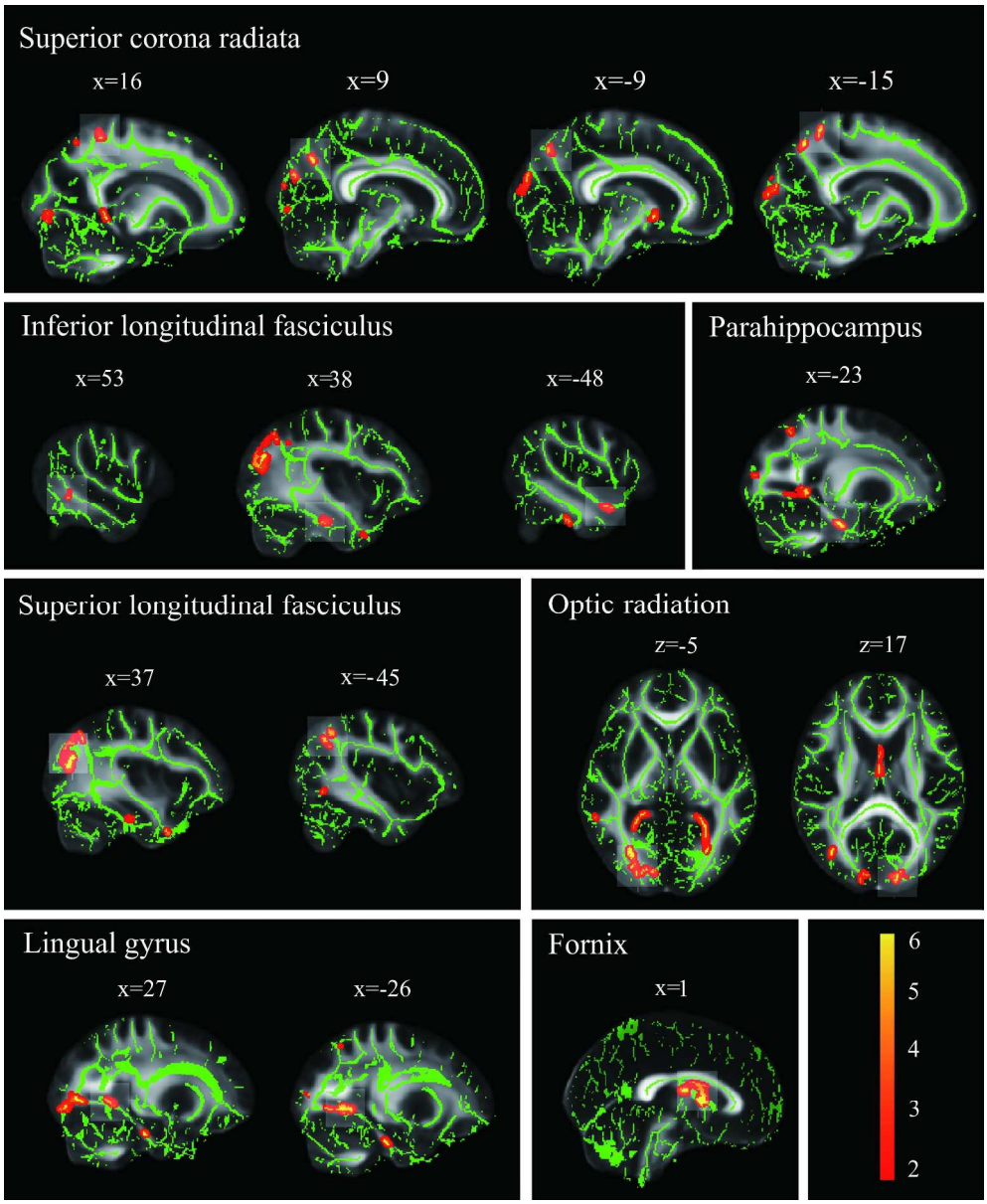

Figure 5 Statistical maps of group comparison of FA value on a voxel-wise basis (results of TBSS). The group's mean FA skeleton (green) was overlaid on the MNI template. The threshold of mean FA skeleton was set at 0.2. COPD patients show significantly lower FA value than healthy controls ($p < 0.05$).

STROBE 2007 (v4) Statement—Checklist of items that should be included in reports of *case-control studies*

Section/Topic	Item #	Recommendation	Reported on page #
Title and abstract	1	(*a*) Indicate the study's design with a commonly used term in the title or the abstract	1
		(*b*) Provide in the abstract an informative and balanced summary of what was done and what was found	2
Introduction			
Background/rationale	2	Explain the scientific background and rationale for the investigation being reported	4
Objectives	3	State specific objectives, including any prespecified hypotheses	4 and 5
Methods			
Study design	4	Present key elements of study design early in the paper	5
Setting	5	Describe the setting, locations, and relevant dates, including periods of recruitment, exposure, follow-up, and data collection	5
Participants	6	*(*a) Give the eligibility criteria, and the sources and methods of case ascertainment and control selection. Give the rationale for the choice of cases and controls	5 and 6
		(*b*) For matched studies, give matching criteria and the number of controls per case	5
Variables	7	Clearly define all outcomes, exposures, predictors, potential confounders, and effect modifiers. Give diagnostic criteria, if applicable	5
Data sources/ measurement	8*	For each variable of interest, give sources of data and details of methods of assessment (measurement). Describe comparability of assessment methods if there is more than one group	*6*
Bias	9	Describe any efforts to address potential sources of bias	
Study size	10	Explain how the study size was arrived at	
Quantitative variables	11	Explain how quantitative variables were handled in the analyses. If applicable, describe which groupings were chosen and why	
Statistical methods	12	(*a*) Describe all statistical methods, including those used to control for confounding	6 - 8
		(*b*) Describe any methods used to examine subgroups and interactions	6 - 8
		(*c*) Explain how missing data were addressed	
		(*d*) If applicable, explain how matching of cases and controls was addressed	
		(*e*) Describe any sensitivity analyses	6 - 8
Results			

Participants	13*	(a) Report numbers of individuals at each stage of study—eg numbers potentially eligible, examined for eligibility, confirmed eligible, included in the study, completing follow-up, and analysed	5
		(b) Give reasons for non-participation at each stage	
		(c) Consider use of a flow diagram	
Descriptive data	14*	(a) Give characteristics of study participants (eg demographic, clinical, social) and information on exposures and potential confounders	17
		(b) Indicate number of participants with missing data for each variable of interest	
Outcome data	15*	Report numbers in each exposure category, or summary measures of exposure	
Main results	16	(*a*) Give unadjusted estimates and, if applicable, confounder-adjusted estimates and their precision (eg, 95% confidence interval). Make clear which confounders were adjusted for and why they were included	9 and 10
		(*b*) Report category boundaries when continuous variables were categorized	
		(*c*) If relevant, consider translating estimates of relative risk into absolute risk for a meaningful time period	
Other analyses	17	Report other analyses done—eg analyses of subgroups and interactions, and sensitivity analyses	
Discussion			
Key results	18	Summarise key results with reference to study objectives	11
Limitations	19	Discuss limitations of the study, taking into account sources of potential bias or imprecision. Discuss both direction and magnitude of any potential bias	
Interpretation	20	Give a cautious overall interpretation of results considering objectives, limitations, multiplicity of analyses, results from similar studies, and other relevant evidence	11-15
Generalisability	21	Discuss the generalisability (external validity) of the study results	
Other information			
Funding	22	Give the source of funding and the role of the funders for the present study and, if applicable, for the original study on which the present article is based	3

*Give information separately for cases and controls in case-control studies and, if applicable, for exposed and unexposed groups in cohort and cross-sectional studies.

Note: An Explanation and Elaboration article discusses each checklist item and gives methodological background and published examples of transparent reporting. The STROBE checklist is best used in conjunction with this article (freely available on the Web sites of PLoS Medicine at http://www.plosmedicine.org/, Annals of Internal Medicine at http://www.annals.org/, and Epidemiology at http://www.epidem.com/). Information on the STROBE Initiative is available at www.strobe-statement.org.

Grey and white matter abnormalities in chronic obstructive pulmonary disease: a case-control study

Journal:	*BMJ Open*
Manuscript ID:	bmjopen-2012-000844.R2
Article Type:	Research
Date Submitted by the Author:	05-Mar-2012
Complete List of Authors:	zhang, haiyan; Department of Physiology and Neurobiology, Medical College of Xiamen University, Xiamen wang, xiaochuan; Department of Neurology, the Affiliated Hospital of Hangzhou Normal University lin, Jianzhong; Magnetic Resonance Center, Zhongshan Hospital, Medical College of Xiamen University sun, Yinchuan; Department of Physiology and Neurobiology, Medical College of Xiamen University, Xiamen huang, Yongxia; Department of Physiology and Neurobiology, Medical College of Xiamen University, Xiamen yang, Tianhe; Magnetic Resonance Center, Zhongshan Hospital, Medical College of Xiamen University zheng, Shili; Departments of Respiratory, Zhongshan Hospital, Medical College of Xiamen University fan, ming; Department of Brain Protection and Plasticity, Institute of Basic Medical Sciences Zhang, Jiaxing; Department of Physiology and Neurobiology, Medical College of Xiamen University
Primary Subject Heading:	Radiology and imaging
Secondary Subject Heading:	Neurology, Respiratory medicine
Keywords:	Adult intensive & critical care < INTENSIVE & CRITICAL CARE, Neuroradiology < NEUROLOGY, Magnetic resonance imaging < RADIOLOGY & IMAGING

Grey and white matter abnormalities in chronic obstructive pulmonary disease: a case-control study

Haiyan Zhang[1#], Xiaochuan Wang[2#], Jianzhong Lin[3], Yinchuan Sun[1], Yongxia Huang[1], Tianhe Yang[3], Shili Zheng[4], Ming Fan [5], Jiaxing Zhang[1]*

1 Department of Physiology and Neurobiology, Medical College of Xiamen University, Xiamen 361005, China;

2 Department of Neurology, the Affiliated Hospital of Hangzhou Normal University, Hangzhou 310015, China;

3 Magnetic Resonance Center, Zhongshan Hospital, Medical College of Xiamen University, Xiamen 361004, China;

4 Departments of Respiratory, Zhongshan Hospital, Medical College of Xiamen University, 361004, Xiamen, China.

5 Department of Brain Protection and Plasticity, Institute of Basic Medical Sciences, Beijing 100850, China

[#], authors with equal contributions

Corresponding author:

Jiaxing Zhang, PhD

Department of Physiology and Neurobiology

Medical College of Xiamen University

Xiamen, 361005, China

Tel: +86-0592-2188-421

Email: zhangjiaxing@xmu.edu.cn

Keywords: Brain, chronic obstructive pulmonary disease, grey matter, magnetic resonance images, white matter

Word count: 2991

ABSTRACT

OBJECTIVES: The irreversible airflow limitation characterised by chronic obstructive pulmonary disease (COPD) causes a decrease in the oxygen supply to the brain. The present study was to investigate brain structural damage in COPD.

DESIGN: Retrospective case-control study. COPD patients and healthy volunteers were recruited. The two groups were matched in age, gender, and educational background.

SETTING: A hospital and a number of communities: they are all located in southern Fujian province, China.

PARTICIPANTS: 25 stable patients and 25 controls were enrolled from December 2009 to May 2011.

METHODS: Using voxel-based morphometry and tract-based spatial statistics based on MRI to analyse grey matter density and white matter fractional anisotropy (FA), respectively, and a battery of neuropsychological tests were performed.

RESULTS: COPD patients (vs. controls) showed decreased grey matter density in the limbic and paralimbic structures, including right gyrus rectus, left precentral gyrus, bilateral anterior and middle cingulate gyri, bilateral superior temporal gyri, bilateral anterior insula extending to Rolandic operculum, bilateral thalamus/pulvinars, and left caudate nucleus. COPD patients (vs. controls) had decreased FA values in the bilateral superior corona radiata, bilateral superior and inferior longitudinal fasciculus, bilateral optic radiation, bilateral lingual gyri, left parahippocampal gyrus, and fornix. Lower FA values in these regions were associated with increased radial diffusivity and no changes of longitudinal diffusivity. COPD patients had poor performances in the Mini Mental State Examination, figure memory, and visual reproduction. GM density in some of the above regions in COPD had positive correlations with arterial blood Po_2 while negative correlations with disease duration, and also,

had positive correlations with visual tasks.

CONCLUSION: We demonstrated that COPD exhibited loss of regional grey matter accompanied by impairment of white matter microstructural integrity, which was associated with disease severity and may underlie the pathophysiological and psychological changes of COPD.

Funding: This work was supported by National Science Foundation of China (Project No. 31071041; 81171324), Bureau of Science and Technology of Hangzhou (20090833B10), and Health Bureau of Zhejiang Province (2009A168).

Competing interests: None.

INTRODUCTION

Chronic obstructive pulmonary disease (COPD) continues to be a major cause of morbidity and mortality. It is increasingly recognised that COPD extends beyond the lung.[1] The irreversible airflow limitation characterised by COPD usually develops arterial oxygen desaturation, which could subsequently result in a decrease in oxygen transport to the brain. Hypoxia during COPD has been previously proven to induce cerebral perfusion decline[2] and metabolic changes.[3-6] Moreover, systematic inflammation[1] may also cause neuronal damages in the brain of COPD patients. In COPD patients, clinical symptoms such as neuropsychological deficits,[7] depression and anxiety,[1] and physical disability[1] have been well documented. Taken together, all these data suggest the presence of brain structural alteration. However, until now, it remains largely uninvestigated.

Voxel-based morphometry (VBM) and Tract-Based Spatial Statistics (TBSS)[8] based on magnetic resonance images (MRI) were adopted to measure grey matter (GM) density and white matter (WM) fibrous microstructure properties in tracts, respectively. VBM is an automatic quantitative volumetric technique over the whole brain using voxel by voxel analysis without prior specification of regions of interest for analysis and it does not rely on arbitrarily predefined structures. Recently, the preprocessing steps of VBM have been improved with the Diffeomorphic Anatomical Registration Through Exponentiated Lie algebra (DARTEL) registration method,[9] which can achieve more accurate inter-subject registration of brain images. TBSS is a recently introduced method, which uses diffusion tensor MR imaging (DTI) to measure differences in fractional anisotropy (FA) between groups. TBSS increases the sensitivity and the interpretability of the results compared with voxel-based approaches based purely on non-linear registration.[8] Moreover, diffusion tensor eigenvalues were also included in the analysis since they can help interpret FA changes in WM tracts by providing information regarding

likely alterations in the proportion of longitudinally vs. obliquely aligned myelinated fibres. The VBM and TBSS methods have been extensively applied in clinical researches, including the evaluation of morphological characteristics of high-altitude residents in our previous study.[10]

Dyspnea is the most common complaint and most disabling symptom in patients with COPD. Functional MRI studies on breathlessness, air hunger, and inspiratory loaded breathing have revealed that a large number of brain regions, including the frontal cortex, parietal cortex, temporal cortex, limbic cortex, cerebellar cortex, and brainstem, were activated by dyspnea.[11] These dyspnea-activated brain regions have been shown to be impaired in congenital central hypoventilation syndrome patients,[12] in obstructive sleep apnea patients,[13] and in high-altitude residents.[10] We therefore hypothesised that COPD patients would have similar cerebral impairment.

METHODS

Subjects

Twenty-five patients were enrolled from December 2009 to May 2011. All patients had undergone a period of 30 to 45 days of in-hospital rehabilitation following an acute exacerbation of COPD. At the time of data collection, patients were in stable condition. Among these patients, 12 discharged patients were recruited during their rest at home and 13 patients were recruited when they were awaiting discharge from hospital. Patients were diagnosed in Zhongshan hospital (Xiamen, China) according to the diagnostic criteria of Global Initiative for Chronic Obstructive Lung Disease (GOLD).[14] Twenty-five healthy volunteers, with comparable age, gender, and educational background, comprised the control group. All the subjects were free from a known history of cerebrovascular accident, heart failure, neurological disorders, OSA, coronary artery disease, diabetes, or other diseases known to

affect cognition. Patients were provided with therapy including inhaled ipratropium bromide, bricanyl, ventoline, and budesonide. Demographic characteristics of the patients and healthy volunteers were listed in Table 1. Procedures were fully explained and all subjects were provided written informed consent before participating in the study. The experimental protocol was approved by the Research Ethics Review Board of Xiamen University.

Physiological and neuropsychological tests

Physiological and neuropsychological tests and activities of daily living (ADL) (score range 14-56)[15] were conducted one day before the MRI scan. Physiological tests include pulse rate and arterial blood pressure measures, arterial blood gas analysis, and pulmonary function measure. Blood samples were taken in the morning between 0700-0730 h. The neuropsychological tests include: (i) the Chinese version of the Mini Mental State Examination (MMSE) measured the general cognitive function. (ii) the visual reproduction test, figure memory test, and digital span forward and backward tasks, which, taken from the Chinese revised version of the Wechsler Memory Scale, were used to measure visual construction ability, visuospatial memory, and short-term working memory, respectively [16]. All data were analysed using SPSS 19.0 (Chicago, IL, USA). Independent t-test measured between-group differences. Statistical significance was set at $p < 0.05$.

MRI data acquisition

Images were acquired on a Siemens Trio Tim 3.0T (Erlangen, Germany) at MRI Research Center (Zhongshan Hospital, Xiamen, China). A 3D structural MRI was acquired from each subject using a T1-weighted MPRAGE sequence (TR/TE = 1900 ms/2.48 ms, FOV = 25 × 25 cm^2, NEX = 1, matrix =

512 × 256, slice thickness = 1.0 mm). Conventional 2D T1 and T2 images were also acquired and examined for any incidental findings. A DTI pulse sequence with single shot diffusion-weighted echo planar imaging (TR/TE = 3600/95 ms, FOV=24 × 24 cm^2, NEX = 2, matrix = 128 × 128, slice thickness = 4.5 mm) was applied sequentially in 30 non-collinear directions (b-value = 1000s/ mm^2) with one scan without diffusion weighting (b = 0s/mm^2). The following data analyses were conducted by two researchers who were blind to the status of subjects.

VBM analysis of 3D T1 images

The 3D T1 images were used for GM analysis using VBM8 toolbox implemented in SPM8 (Wellcome Department of Imaging Neuroscience, University College London, London, UK). The following processing steps were carried out: (i) the images were inspected and set at the anterior commissure. Each reorientated image was segmented into GM, WM and CSF in native space and procrustes aligned GM images were generated by a rigid transformation. (ii) the DARTEL registration method was used to create a study-specific template by using the aligned images from all the patients and controls to improve inter-subject registration of structural images.[9] The procedure implicated in six iterations, which began with the averaging of aligned data to generate an original template. Then, the first iteration of the registration was completed on each subject and a new template was created. After this, the second iteration began. When six iterations were finished, the template was generated, which was the average of the DARTEL registered data. During iterations, all images were warped to the template yielding a series of flow fields that parameterised deformations. (iii) the normalised images were transformed into MNI space. These GM images were then smoothed using a Gaussian kernel of 8 mm full-width at half-maximum. Independent t-tests were performed to examine between-group differences.

The statistical parametric map was generated with the voxel level threshold at $t > 3.7734$, $p < 0.01$ (FDR correction with gender, age, education, and total intracranial volume as covariates).

To analysed the correlation of GM image values with cognitive or physiological measurement, the following steps were first taken: (1) Regions-of-interests were created for clusters showing differences between groups; (2) using these Regions-of-interests masks, the GM values were extracted from each individual's normalised and smoothed GM maps. Then the correlations were analysed using SPSS. Statistical significance was set at $p < 0.05$, with gender, age, and education as covariates.

TBSS analysis of DTI

DCM2MII was used to convert diffusion tensor images from the proprietary scanner format to the NIFTI format. Then the images were processed using the FSL 4.1.5 software package (http://www.fmrib.ox.ac.uk/fsl/). The images were realigned to the b-value (b0) image by affine transformations using FMRIB's diffusion toolbox (FDT) [17] to minimise distortions and reduce head motion artifacts. In order to remove non-brain tissue components and background noise, a brain mask was created from the first b0 image, and then applied in the DTI to extract brain voxels using Brain Extraction Tool (BET). After these processes, using DTIFit within the FDT, the images were calculated to get the FA, $\lambda 1$ (longitudinal diffusivity) (the magnitude of diffusion along the principal diffusion direction), and $\lambda 23$ (radial diffusivity) (the magnitude of diffusion in the two orthogonal directions perpendicular to the principal diffusion direction) maps. The whole brain voxel-wise statistic analysis of the FA images was performed using TBSS in FSL.[7] TBSS processing includes the following steps: (i) align the FA images of all subjects to a template which was arbitrarily selected from those FA images by nonlinear registrations; (ii) transform all the aligned FA images into $1\times1\times1$ mm^3 MNI152 space by

affine registrations to remove the effect of cross-subject spatial variability that remains after the non-linear registration; (iii) create the mean FA image and filter to retain only the centre of the WM tracts, with the threshold FA ≥ 0.20, and successfully exclude voxels, which consisted of GM or CSF in the majority of subjects, so as to create the mean FA skeleton.[8] (iv) project individual subjects' FAs onto mean FA skeleton. (v) following these steps, data was fed into voxel-wise cross-subject statistical analyses. In all cases, the null distribution was built up over 5000 permutations, with significance analysed using independent t-tests at $p < 0.05$ levels, uncorrected for multiple comparisons. We determined the anatomic localisation of each cluster by means of the FSL atlas tool, which incorporates several anatomic templates, including the Harvard-Oxford Cortical Structural Atlas, Harvard-Oxford Subcortical Structural Atlas, Talairach Daemon Labels, and MNI Structural Atlas.

Within the cluster of changed FA, mean λ1 and λ23 values were extracted from each individual's λ1 and λ23 maps. Values were analysed using SPSS. ANOVA statistic was used to identify the group differences for these distinct brain locations. Statistical significance was set at $p < 0.05$.

RESULTS

Physiological and behavioral findings (Table 2)

Compared with the controls, independent t-test showed that COPD patients had significant decreases in arterial blood Sao_2 and Po_2, and increases in arterial blood Pco_2 and heart rate. COPD patients had significantly lower values in one second over forced vital capacity (FVC), forced expiratory volume (FEV), and FEV1/FVC values and higher respiratory rate. The disease staging categories of COPD patients based on FEV1% predicted were as follows: FEV1 = 82 % predicted, n = 1; 54.9% ≤ FEV1 < 78% (64.9±7.6) predicted, n = 8; 31.9% ≤ FEV1 < 48.4% (42.0±5.4) predicted, n = 7; FEV1 < 29.9%

(26.2±2.9) predicted, n = 9. COPD patients had significantly lower scores in ADL, MMSE test, visual reproduction, and figure memory.

GM density

No subject from either group showed visible abnormalities on T1-weighted structural images. VBM analysis showed that COPD patients had decreased GM densities compared with healthy controls in the right gyrus rectus, left precentral gyrus, bilateral anterior and middle cingulate gyri, bilateral superior temporal gyri, bilateral anterior insula extending to Rolandic operculum (base of the pre- and post-central gyri), bilateral thalamus/pulvinars, and left caudate nucleus (cluster size > 100 voxels) (Fig. 1-4, Table 3).

FA, longitudinal diffusivity, and radial diffusivity in relation to COPD

Whole-brain voxel-wise statistic analysis showed COPD patients had significantly lower FA in a broad range of brain regions compared with controls (Fig. 5, Table 4). The significantly affected regions (clusters size > 40 voxels) included the superior corona radiata (corresponding to bilateral precuneus and bilateral superior parietal lobules), superior longitudinal fasciculus (bilateral supramarginal gyri), inferior longitudinal fasciculus (left superior temporal gyrus, right middle temporal gyrus, and fusiform gyrus), bilateral optic radiation, bilateral lingual gyri, left parahippocampal gyrus, and fornix.

Lower FA values in these regions were associated with increased radial diffusivity and no changes of longitudinal diffusivity in COPD patients vs. controls (Table 4).

Correlations between MRI measurement and disease severity

The correlations were listed in Table 5. In COPD patients, partial correlation (controlling for disease duration, FEV1/FVC, age, education, and gender) revealed GM density in the bilateral anterior cingulate cortex, left superior temporal cortex, bilateral insula/superior temporal/Rolandic Operulum, bilateral thalamus/Pulvinar, and left caudate nucleus had positive correlations with arterial blood Po_2. Partial correlation (controlling for Po_2, FEV1/FVC, age, education, and gender) revealed GM density in the bilateral anterior cingulate cortex, right insula/superior temporal/Rolandic Operulum, and right thalamus/Pulvinar had negative correlations with disease duration. Partial correlation (controlling for age, education, and gender) analysis showed that the GM density in the left superior temporal lobes and left insula/superior temporal/Rolandic Operculum in COPD patients was significantly correlated with figure memory score and the GM density in left precentral gyrus and left thalamus/Pulvinar in COPD patients correlated significantly with visual reproduction.

DISCUSSION

Our present study revealed that COPD patients had decreased regional GM density confined to the limbic and paralimbic structures. GM density in impaired regions in COPD patients had significant positive correlation with arterial blood Po_2 and negative correlation with disease duration. The decreased WM FA value with increased radial diffusivity value was detected mainly in the visual cortex of the occipital lobe, the posterior parietal lobe as well as the temporal lobe. Decreased FA was associated with compromised myelin structure, changes in axonal morphologic structure, and altered interaxonal spacing of fibre bundles.[18] Radial diffusivity measures motion of water molecules perpendicular to fibres and an increase of radial diffusivity is interpreted as abnormalities in myelinated membranes.[19] Consequently, decreased FA and increased radial diffusivity in COPD indicated the

impairment of WM microstructural integrity.

Previously, Borson et al.[6] only measured the volume of hippocampus in COPD patients using region-of-interest analysis and did not find significant change. The impaired brain regions in COPD have also been found in other chronic hypoxic diseases. For example, decrease in GM volume/concentration in the gyrus rectus, precentral gyrus, anterior cingulate cortex, multiple sites within the temporal lobes, insular cortex, thalamus, and caudate nucleus were detected in patients with obstructive sleep apnea.[13] Impairments of WM microstructure in the temporal lobe, parietal lobe, fornix, and corona radiata were found in patients with congenital central hypoventilation syndrome.[12] In our previous study, the decrease in GM volume in the anterior insula, anterior cingulate cortex, and precentral cortex were found in high-altitude residents.[10]

GM density in impaired regions in COPD patients had a strongly positive correlation with the arterial blood Po_2, which suggested the impairment in GM may result from low blood oxygen. Moreover, the GM density in some impaired regions showed negative correlations with disease duration. It is already known that hypoxia can induce metabolic decreases[3-5] and cerebral perfusion decline[2] in COPD. In addition, COPD patients often suffer from systemic inflammation, which can exacerbate neuronal injury.[1] A greater proportion of regions showing GM loss located in limbic/paralimbic cortex in COPD patients may be due to the fact that phylogenetically older regions of the brain showed sharper vascular responses to hypoxia than evolutionary younger regions.[20]

A larger cortical network including the anterior insula and anterior cingulate cortex underlie the perception of dyspnea[11] and these regions play an important role in regulating the cardiovascular system.[21] Posterior thalamus was implicated in suppressing the ventilatory response to hypoxia.[22] Hippocampus has been proved to control arterial pressure and heart rate.[23] Thus the morphological

impairments in these regions may play a role in respiratory and cardiovascular disturbances, such as higher heart rate and higher respiratory rate, in COPD patients tested in our study.

In the present study, COPD patients had poorer performance in MMSE, visuospatial memory, and visual construction task. These results were consistent with those found in previous studies in COPD patients.[7] In line with the present findings of COPD, we previously found that long-time living in mild high-altitude hypoxic environment only impaired cognitive performances confined to visual reproduction and short-time complex figure memory.[24] In our present study, the decreases in GM density in the frontal precentral cortex, insula/superior temporal cortex/Rolandic Operculum, and thalamus/pulvinar may be responsible for the performance deficit in visual-related tasks since the GM density in these areas showed a significant positive correlation with figure memory or visual reproduction score. The following data support our findings: (i) Recent research has identified the inferior frontal cortex served as a source of top-down modulation underlying attention to visual features.[25] (ii) Studies on patients using fMRI and PET demonstrated Rolandic operculum as one of the visual structures.[26] (iii) The pulvinar region of the thalamus is known to project to posterior parietal lobe and inferior temporal lobe. The pulvinar has been implicated in various visual functions in lesion studies.[27] Declines in memory and executive function make contributions to declines in ADL.[28] Visual construction tasks reflect executive function. Therefore, the decreases in GM density in the above regions that relate to visual construction may also be responsible for ADL deficits.

Our present study found the impairments of WM limited to the pathways of visual processing, including optic radiation, posterior parietal lobe (superior parietal lobule, supramarginal gyrus, and precuneus), and the inferior temporal fusiform and lingual gyri. Visual information enters the primary visual cortex via optic radiation to the visual cortex. Cortical areas along the posterior parietal 'dorsal

stream' are primarily concerned with spatial localisation and directing attention, while cortical areas along the inferior temporal 'ventral stream' are mainly concerned with the recognition and identification of visual stimuli.[29] COPD also showed impaired WM in the middle temporal gyrus. Middle temporal cortex is important for the long-term buildup of perceptual memory for ambiguous motion stimuli.[30] Based on the above data, our findings in WM may also clarify the mechanisms underlying the deficit in visual-related tasks. In addition, impaired WM in input and output fibres of hippocampus (fornix) may be related to the deficit in MMSE. Previous study on patients with Alzheimer's disease found the volumes of hippocampus were significantly reduced and the volumes of the left hippocampus correlated significantly with the MMSE score.[31] The limitation of our study is the weak statistical power of FA value analysis, because the results obtained in the TBSS analysis could not survive multiple comparison correction.

Conclusions

In summary, we first demonstrated that COPD extended beyond the lung to the brain, with the decrease of regional GM density accompanied by impairment in the WM microstructural integrity. Our findings suggest significant participation of these structures in responding to hypoxic challenges, which include cardiovascular and air-hunger components. The brain structural changes may also underlie the psychological and mood changes of COPD.

Authors' contributions

Haiyan Zhang: contributed to conception and design, the accuracy of the data analysis, drafting the article, and final approval of the version to be published.

Xiaochuan Wang: contributed to the study design, revising the article critically for important intellectual content, and final approval of the version to be published.

Jianzhong Lin: contributed to acquisition of data, revising the article critically for important intellectual content, and final approval of the version to be published.

Yingchun Sun: contributed to acquisition of data, revising the article critically for important intellectual content, and final approval of the version to be published.

Yongxia Huang: contributed to acquisition of data, revising the article critically for important intellectual content, and final approval of the version to be published.

Tianhe Yang: contributed to acquisition of data, revising the article critically for important intellectual content, and final approval of the version to be published.

Shili Zheng: contributed to acquisition of data, revising the article critically for important intellectual content, and final approval of the version to be published.

Ming Fan: contributed to acquisition of data, revising the article critically for important intellectual content, and final approval of the version to be published.

Jiaxing Zhang: contributions to conception and design, acquisition of data, and interpretation of data; drafting the article and revising it critically for important intellectual content; and final approval of the version to be published.

Table 1 Demographic characteristics of the patients with COPD and healthy volunteers

	COPD patients	Controls	p
Number of subjects	25	25	
Gender (female) (%)	16	16	
Age (years) (mean ± SD)	69.2 ± 8.1 (58 - 84)	67.96 ± 8.0 (57 - 86)	0.59
Education (years) (mean ± SD)	6.7 ± 3.9	7.5 ± 5.0	0.53
Family history of COPD (%)	4	-	
Disease duration (years)	7.0 ± 5.7	-	
Actual smokers (%)	44	40	0.86

Table 2 Physiological and psychological characteristics

	COPD patients	Controls	*P*
BMI (kg/m^2)	20.8 ± 3.9	22.6 ± 2.6	0.081
ADL	20.12 ± 6.5	14.6 ± 1.52	<0.001
Heart rate	92.4 ± 16.2	70.9 ± 8.94	<0.001
Blood pressure (mmHg)			
systolic pressure	136.1±19.1	136.5 ± 18.0	0.940
diastolic pressure	81.8 ± 10.7	77.5 ± 14.5	0.307
Hematological measurements			
Sao_2 (%)	94.0 ± 4.2	97.0 ± 1.3	0.003
Po_2 (mmHg)	79.9 ± 23.3	98.5 ± 11.3	0.006
Pco_2 (mmHg)	48.1 ± 6.0	39.8 ± 3.0	<0.001
pH	7.37 ± 0.06	7.36 ± 0.01	0.731
Pulmonary Function testing			
Respiratory rate (breaths/min)	23.5 ± 6.0	16.9 ± 5.5	0.003
FVC (% predicted)	66.6 ± 17.2	96.1 ± 14.7	<0.001
FEV1 (% predicted)	43.4 ± 16.4	97.5 ± 16.9	<0.001
FEV1/ FVC (%)	50.31 ± 10.7	80.0 ± 8.32	<0.001
Cognitive tests			
MMSE	23.3 ± 3.4	25.8 ± 2.1	0.021
Digit Span			

Forward task	7.0 ± 1.6	7.7 ± 1.4	0.125
Backward task	4.1 ± 1.9	4.3 ± 1.5	0.612
Visual reproduction	8.2 ± 3.4	10.3 ± 3.0	0.031
Figure memory	10.5 ± 3.0	12.4 ± 1.9	0.010

ADL, activities of daily living; BMI, body mass index; FEV1, forced expired volume in one second; FVC, forced vital capacity; MMSE, Mini Mental State Examination. Data are mean ± SD.

Table 3 Regional information of decreased grey matter density (cluster size > 100 voxels) in COPD patients compared with healthy controls

Area	**Volume (mm^3)**	**Brodmann areas**	**MNI coordinate**			**t-score (peak)**
			x	**y**	**z**	
Rectus_R	118	11	9	39	-20	4.31
Precentral_L	100	6	-51	-5	33	4.95
Cingulum_Ant_R	485	32	8	38	17	5.88
Cingulum_Ant_L	212	32	-8	38	18	4.49
Cingulum_Mid_R	157	24	6	-9	42	4.87
Cingulum_Mid_L	136	24	-6	-9	41	4.91
Temporal_Sup_ L	280	22/42	-60	-33	3	4.99
Temporal_Sup/ Rolandic_Oper _L	837	22	-57	-14	10	4.91
Insula/Temporal_Sup/ Rolandic_Oper _R	2821	13/22/47	44	11	-5	5.15
Insula/Temporal_Sup/ Rolandic_Oper _L	1551	13/22/47	-33	12	-15	4.48
Thalamus/Pulvinar_L	1270		-12	-30	3	6.46
Thalamus/Pulvinar_R	2210		12	-26	8	5.29

Caudate_L	212	-9	14	14	4.19

Table 4 Main regions showing FA, λ1, λ23 values in COPD patients compared with healthy controls

MNI (peak)			Voxels	White matter	Corresponding cortical area	FA value		λ1 (×10^3 mm^2/s)		λ23 (×10^3 mm^2/s)	
x	y	z	(mm^3)	tract		COPD	Control	COPD	Control	COPD	Control
1	10	16	240	Fornix	Fornix	0.248(0.067)	0.289(0.073)	2.586(0.314)	2.406(0.0321)	1.809(0.295)	1.577(0.262)*
-26	-69	1	191	Lingual gyrus	Left lingual gyrus	0.259(0.042)	0.283(0.046)	1.450(0.240)	1.370(0.224)	0.992(0.185)	0.896(0.168)*
27	-53	3	147	Lingual gyrus	Right lingual gyrus	0.265(0.065)	0.290(0.056)	1.381(0.239)	1.346(0.227)	0.955(0.242)	0.891(0.215)*
-23	-19	-24	77	Parahippocampus	Left parahippocampus	0.268(0.042)	0.319(0.046)	1.234(0.057)	1.189(0.052)	0.869(0.148)	0.771(0.125)*
38	-24	-24	77	fusiform gyrus	Right fusiform gyrus	0.231(0.037)	0.248(0.046)	1.053(0.063)	1.094(0.073)	0.774(0.030)	0.723(0.032)*
-10	-91	17	204	Optic radiation	Left occipital cortex	0.234(0.043)	0.277(0.041)	1.037(0.038)	1.020(0.031)	0.752(0.063)	0.693(0.051)*
25	-86	-5	200	Optic radiation	Right occipital cortex	0.369(0.099)	0.409(0.122)	1.171(0.014)	1.177(0.171)	0.649(0.057)	0.601(0.071)*
-9	-72	45	94	SCR	Left precuneus	0.283(0.053)	0.317(0.056)	1.099(0.032)	1.069(0.041)	0.726(0.075)	0.665(0.065)*
9	-66	37	57	SCR	Right precuneus	0.251(0.030)	0.280(0.044)	1.044(0.032)	1.018(0.023)	0.868(0.073)	0.731(0.084)*
-15	-51	62	57	SCR	Left superior parietal lobule	0.267(0.043)	0.294(0.043)	1.130(0.051)	1.082(0.025)	0.724(0.039)	0.671(0.045)*
16	-45	64	66	SCR	Right superior parietal lobule	0.251(0.043)	0.294(0.051)	1.176(0.117)	1.107(0.094)	0.805(0.056)	0.762(0.056)*

-45	-53	31	44	SLF	Left supramarginal gyrus	0.221(0.027)	0.239(0.026)	1.088(0.020)	1.076(0.040)	0.935(0.090)	0.873(0.071)*
37	-68	21	63	SLF	Right supramarginal gyrus	0.220(0.025)	0.237(0.025)	1.116(0.039)	1.090(0.052)	0.773(0.076)	0.715(0.007)*
-48	0	-16	43	ILF	Left superior temporal gyrus	0.244(0.013)	0.270(0.021)	1.060(0.030)	0.984(0.015)	0.758(0.025)	0.714(0.037)*
53	-46	-6	41	ILF	Right middle temporal gyrus	0.206(0.016)	0.241(0.024)	1.025(0.016)	1.006(0.021)	1.605(0.167)	1.340(0.139)*

ILF, inferior longitudinal fasciculus; SCR, superior corona radiata; SLF, superior longitudinal fasciculus. Data are presented as means (SD). *p<0.05.

Table 5 Correlations of grey matter density in impaired regions with Po_2, disease duration, and cognitive performances in patients with COPD

Area	**Po_2 (patients)**	**Disease duration (patients)**	**Cognitive performances (patients + controls)**	
			figure memory	**visual reproduction**
Precentral_L				r=0.306, p=0.028
2Cingulum_Ant_R	r=0.530, p=0.021	r=-0.471, p=0.038		
1Cingulum_Ant_L	r=0.744, p=0.001	r=-0.476, p=0.036		
Cingulum_Mid_R				
Cingulum_Mid_L				
11Temporal_Sup_L	r=0.713, p=0.001		r=0.511, p=0.001	
Temporal_Sup/ Rolandic_Oper _L				
6Insula/Temporal_Sup/ Rolandic_Oper _R	r=0.615, p=0.007			

7Insula/Temporal_Sup/Rolandic_Oper _L	r=0.656, p=0.004		r=0.498, p=0.001	
9Thalamus/Pulvinar_L	r=0.487, p =0.033	r=-0.474, p=0.037		r=0.284, p =0.044
8Thalamus/Pulvinar_R	r=0.502, p =0.028	r=-0.517, p=0.024		
5Caudate_L	r=0.550, p=0.017			

REFERENCES

1. Barnes PJ. Chronic obstructive pulmonary disease: effects beyond the lungs. *PLoS Med* 2010; 7:e1000220.
2. Ortapamuk H, Naldoken S. Brain perfusion abnormalities in chronic obstructive pulmonary disease: comparison with cognitive impairment. *Ann Nucl Med* 2006; 20:99-106.
3. Shim TS, Lee JH, Kim SY, *et al*. Cerebral metabolic abnormalities in COPD patients detected by localized proton magnetic resonance spectroscopy. *Chest* 2001; 120:1506-13.
4. Sicard KM, Duong TQ. Effects of hypoxia, hyperoxia, and hypercapnia on baseline and stimulus-evoked BOLD, CBF, and CMRO2 in spontaneously breathing animals. *Neuroimage* 2005; 25:850-8.
5. Sinha S, Kumar V, Jagannathan NR, *et al*. Proton magnetic resonance spectroscopy of brain to study the cerebral metabolic abnormalities in COPD patients: a case control study in north India. *Indian J Chest Dis Allied Sci* 2009; 51:15-9.

6. Borson S, Scanlan JM, Friedman S, *et al*. Modeling the impact of COPD on the brain. *International Journal of Chronic Obstructive Pulmonary Disease* 2008; 3: 429-34.

7. Dodd JW, Getov SV, Jones PW. Cognitive function in COPD. *Eur Respir J* 2010; 35:913-22.

8. Smith SM, Jenkinson M, Johansen-Berg H, *et al*. Tract-based spatial statistics: voxelwise analysis of multi-subject diffusion data. *Neuroimage* 2006; 31:1487-505.

9. Ashburner J. A fast diffeomorphic image registration algorithm. *Neuroimage* 2007; 38:95-113.

10. Zhang J, Yan X, Shi J, *et al*. Structural modifications of the brain in acclimatization to high-altitude. *PLoS One* 2010; 5:e11449.

11. von Leupoldt A, Dahme B. Cortical substrates for the perception of dyspnea. *Chest* 2005; 128:345-54.

12. Kumar R, Macey PM, Woo MA, *et al*. Diffusion tensor imaging demonstrates brainstem and cerebellar abnormalities in congenital central hypoventilation syndrome. *Pediatr Res* 2008; 64:275-80.

13. Joo EY, Tae WS, Lee MJ, *et al*. Reduced brain gray matter concentration in patients with obstructive sleep apnea syndrome. *Sleep* 2010; 33:235-41.

14. Pauwels RA, Buist AS, Calverley PM, *et al*. Global strategy for the diagnosis, management, and prevention of chronic obstructive pulmonary disease. NHLBI/WHO Global Initiative for Chronic Obstructive Lung Disease (GOLD) Workshop summary. *Am J Respir Crit Care Med* 2001; 163:1256-76.

15. Lawton MP, Brody EM. Assessment of older people: self-maintaining and instrumental activities of daily living. *Gerontologist* 1969; 9:179-86.

16. Gong YX. Manual for the Wechsler Memory Scale-Revised. Hunan Medical University. Changsha,

Hunan, China. 1989.

17. Jenkinson M, Smith S. A global optimisation method for robust affine registration of brain images. *Med Image Anal* 2001; 5:143-56.

18. Beaulieu C. The basis of anisotropic water diffusion in the nervous system - a technical review. *NMR Biomed* 2002; 15:435-55.

19. Song SK, Sun SW, Ramsbottom MJ, *et al*. Dysmyelination revealed through MRI as increased radial (but unchanged axial) diffusion of water. *Neuroimage* 2002; 17:1429-36.

20. Binks AP, Cunningham VJ, Adams L, *et al*. Gray matter blood flow change is unevenly distributed during moderate isocapnic hypoxia in humans. *J Appl Physiol* 2008; 104:212-7.

21. Nagai M, Hoshide S, Kario K. The insular cortex and cardiovascular system: a new insight into the brain-heart axis. *J Am Soc Hypertens* 2010; 4:174-82.

22. Teppema LJ, Dahan A. The ventilatory response to hypoxia in mammals: mechanisms, measurement, and analysis. *Physiol Rev* 2010; 90:675-754.

23. Macefield VG, Gandevia SC, Henderson LA. Neural sites involved in the sustained increase in muscle sympathetic nerve activity induced by inspiratory capacity apnea: a fMRI study. *J Appl Physiol* 2006; 100:266-73.

24. Zhang J, Liu H, Yan X, *et al*. Minimal effects on human memory following long-term living at moderate altitude. *High Alt Med Biol* 2011; 12:37-43.

25. Zanto TP, Rubens MT, Bollinger J, *et al*. Top-down modulation of visual feature processing: the role of the inferior frontal junction. *Neuroimage* 2010; 53:736-45.

26. Fried I, Nenov VI, Ojemann SG, *et al*. Functional MR and PET imaging of rolandic and visual cortices for neurosurgical planning. *J Neurosurg* 1995; 83:854-61.

27. Arend I, Machado L, Ward R, *et al*. The role of the human pulvinar in visual attention and action: evidence from temporal-order judgment, saccade decision, and antisaccade tasks. *Prog Brain Res* 2008; 171:475-83.

28. Tomaszewski Farias S, Cahn-Weiner DA, Harvey DJ, *et al*. Longitudinal changes in memory and executive functioning are associated with longitudinal change in instrumental activities of daily living in older adults. *Clin Neuropsychol* 2009; 23:446-61.

29. Itti L, Koch C. Computational modelling of visual attention. *Nat Rev Neurosci* 2001; 2:194-203

30. Brascamp JW, Kanai R, Walsh V, *et al*. Human middle temporal cortex, perceptual bias, and perceptual memory for ambiguous three-dimensional motion. *J Neurosci* 2010; 30:760-6.

31. Laakso MP, Soininen H, Partanen K, *et al*. Volumes of hippocampus, amygdala and frontal lobes in the MRI-based diagnosis of early Alzheimer's disease: correlation with memory functions. *J Neural Transm Park Dis Dement Sect* 1995; 9:73-86.

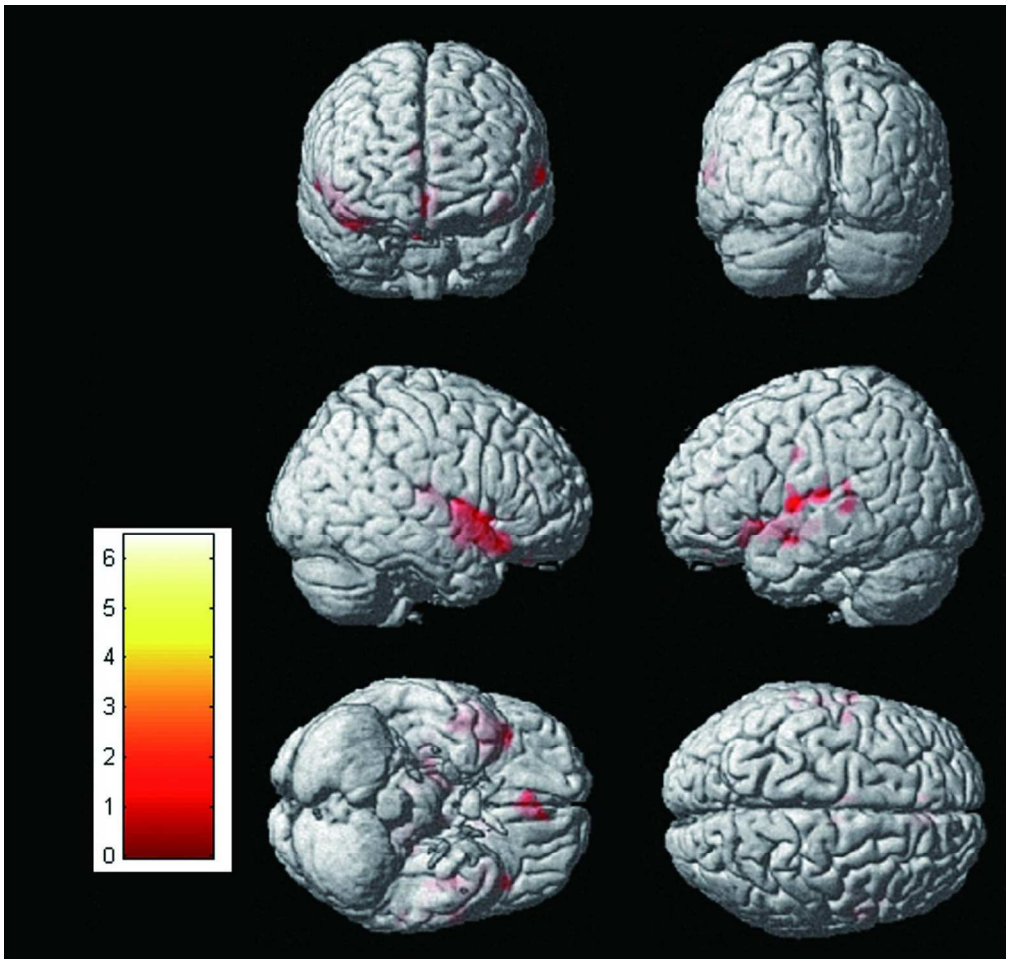

Figure 1 A statistical parametric map for grey matter density reduced in COPD patients vs. healthy controls (pFDR_corrected< 0.01) overlaid on the MNI template.

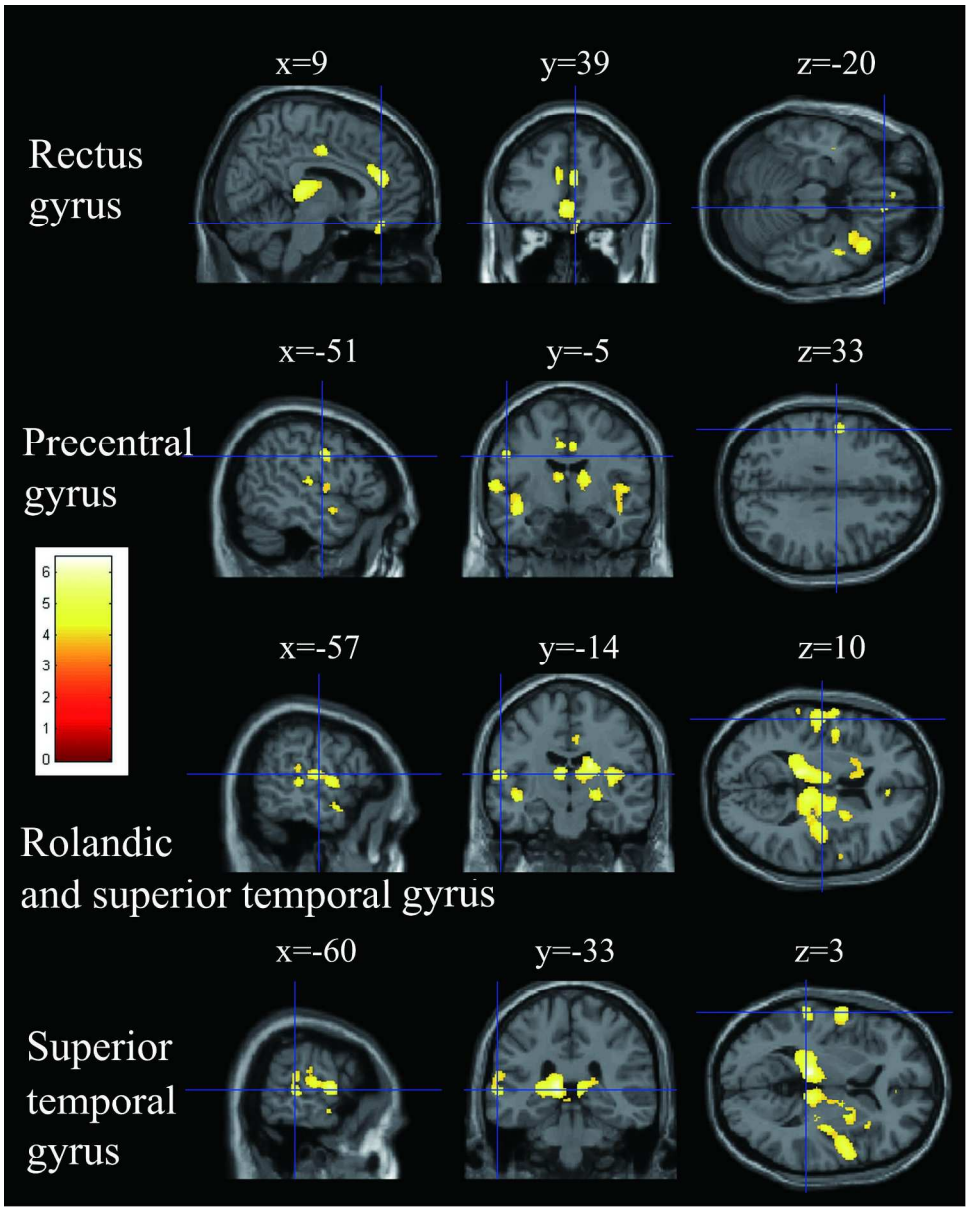

Figure 2 Grey matter density decrease in COPD patients vs. healthy controls. Three-dimensional slices depicting regions showing reduced grey matter in the right gyrus rectus, left precentral gyrus, left Rolandic operculum and superior temporal gyrus overlaid on a T1-weighted MRI anatomical image in the MNI template.

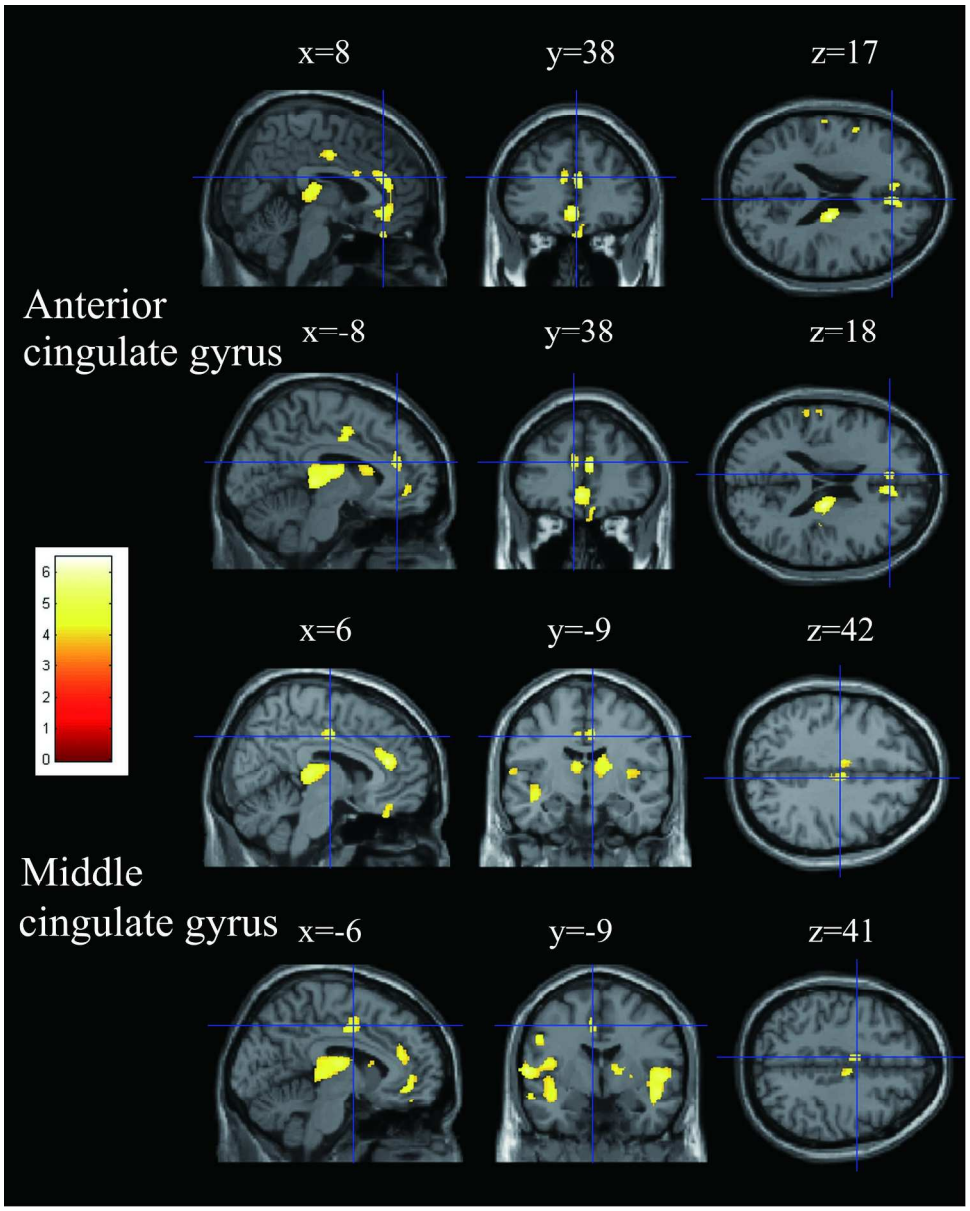

Figure 3 Grey matter density decrease in COPD patients vs. healthy controls. Three-dimensional slices depicting regions showing reduced grey matter in the bilateral anterior and middle cingulate gyri overlaid on a T1-weighted MRI anatomical image in the MNI template.

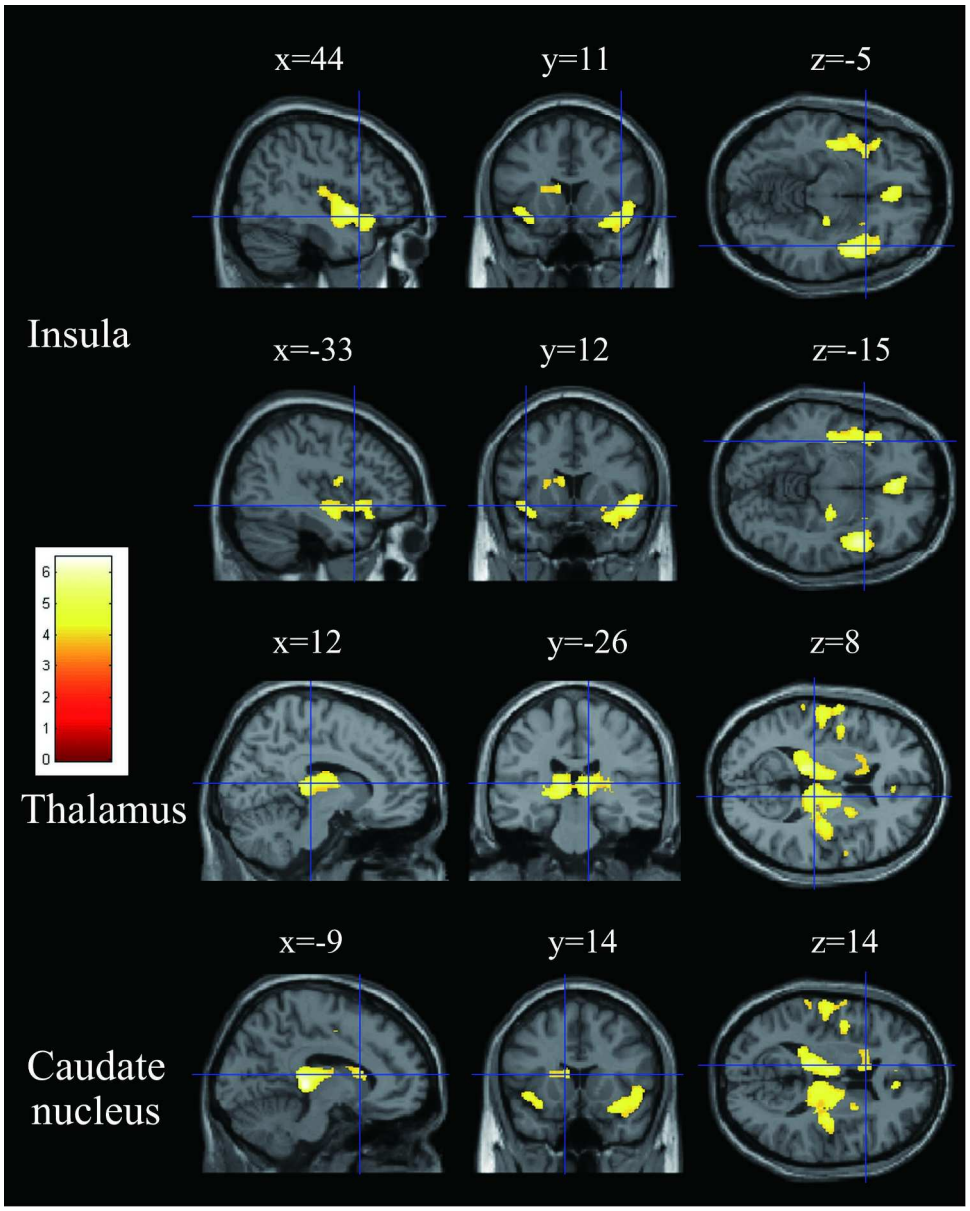

Figure 4 Grey matter density decrease in COPD patients vs. healthy controls. Three-dimensional slices depicting regions showing reduced grey matter in the bilateral insula, bilateral thalamus, and left caudate nucleus overlaid on a T1-weighted MRI anatomical image in the MNI template.

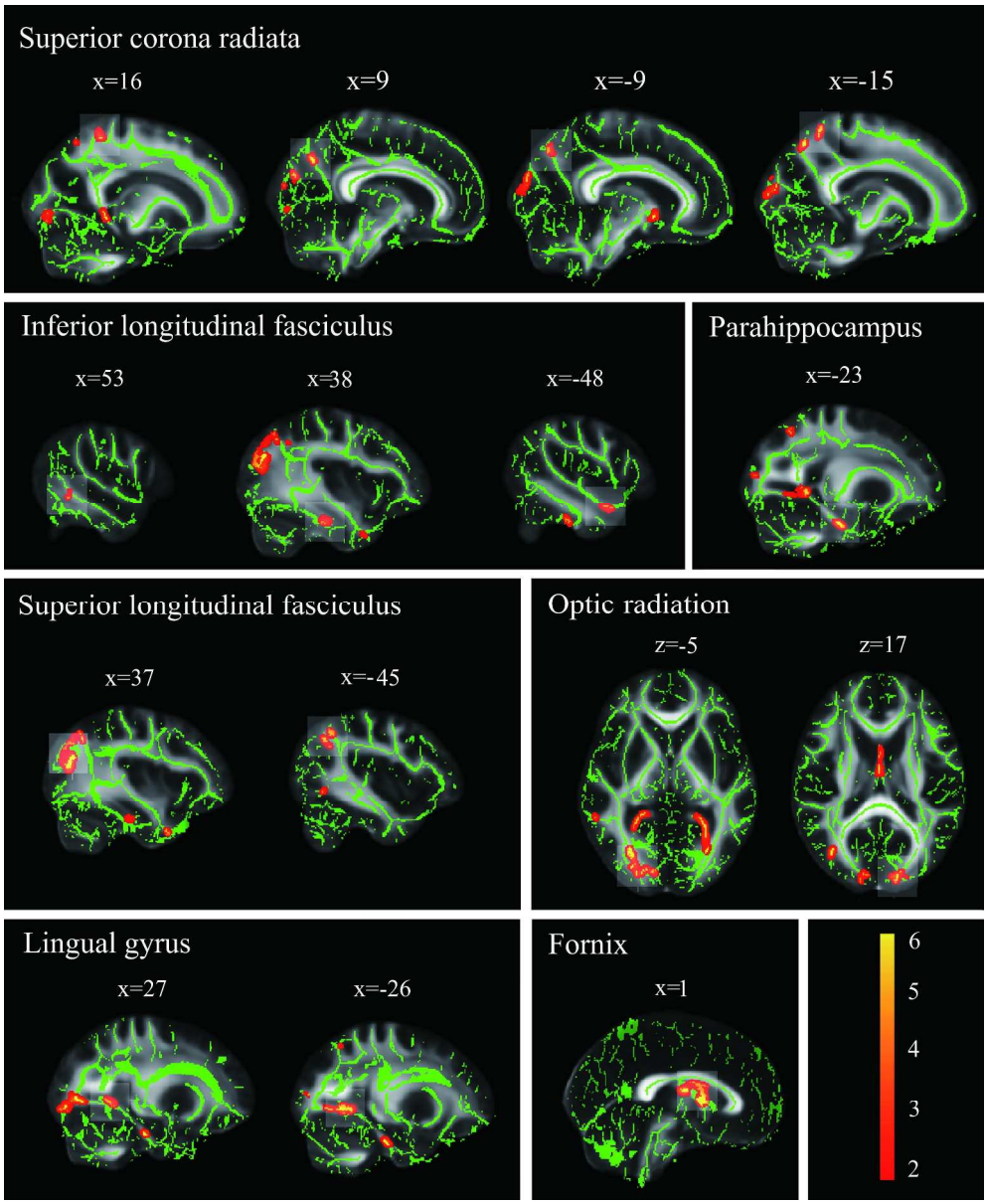

Figure 5 Statistical maps of group comparison of FA value on a voxel-wise basis (results of TBSS). The group's mean FA skeleton (green) was overlaid on the MNI template. The threshold of mean FA skeleton was set at 0.2. COPD patients show significantly lower FA value than healthy controls ($p < 0.05$).

STROBE 2007 (v4) Statement—Checklist of items that should be included in reports of *case-control studies*

Section/Topic	Item #	Recommendation	Reported on page #
Title and abstract	1	(*a*) Indicate the study's design with a commonly used term in the title or the abstract	1
		(*b*) Provide in the abstract an informative and balanced summary of what was done and what was found	2
Introduction			
Background/rationale	2	Explain the scientific background and rationale for the investigation being reported	4
Objectives	3	State specific objectives, including any prespecified hypotheses	4 and 5
Methods			
Study design	4	Present key elements of study design early in the paper	5
Setting	5	Describe the setting, locations, and relevant dates, including periods of recruitment, exposure, follow-up, and data collection	5
Participants	6	*(*a) Give the eligibility criteria, and the sources and methods of case ascertainment and control selection. Give the rationale for the choice of cases and controls	5 and 6
		(*b*) For matched studies, give matching criteria and the number of controls per case	5
Variables	7	Clearly define all outcomes, exposures, predictors, potential confounders, and effect modifiers. Give diagnostic criteria, if applicable	5
Data sources/ measurement	8*	For each variable of interest, give sources of data and details of methods of assessment (measurement). Describe comparability of assessment methods if there is more than one group	*6*
Bias	9	Describe any efforts to address potential sources of bias	
Study size	10	Explain how the study size was arrived at	
Quantitative variables	11	Explain how quantitative variables were handled in the analyses. If applicable, describe which groupings were chosen and why	
Statistical methods	12	(*a*) Describe all statistical methods, including those used to control for confounding	6 - 8
		(*b*) Describe any methods used to examine subgroups and interactions	6 - 8
		(*c*) Explain how missing data were addressed	
		(*d*) If applicable, explain how matching of cases and controls was addressed	
		(*e*) Describe any sensitivity analyses	6 - 8
Results			

Participants	13*	(a) Report numbers of individuals at each stage of study—eg numbers potentially eligible, examined for eligibility, confirmed eligible, included in the study, completing follow-up, and analysed	5
		(b) Give reasons for non-participation at each stage	
		(c) Consider use of a flow diagram	
Descriptive data	14*	(a) Give characteristics of study participants (eg demographic, clinical, social) and information on exposures and potential confounders	17
		(b) Indicate number of participants with missing data for each variable of interest	
Outcome data	15*	Report numbers in each exposure category, or summary measures of exposure	
Main results	16	(*a*) Give unadjusted estimates and, if applicable, confounder-adjusted estimates and their precision (eg, 95% confidence interval). Make clear which confounders were adjusted for and why they were included	9 and 10
		(*b*) Report category boundaries when continuous variables were categorized	
		(*c*) If relevant, consider translating estimates of relative risk into absolute risk for a meaningful time period	
Other analyses	17	Report other analyses done—eg analyses of subgroups and interactions, and sensitivity analyses	
Discussion			
Key results	18	Summarise key results with reference to study objectives	11
Limitations	19	Discuss limitations of the study, taking into account sources of potential bias or imprecision. Discuss both direction and magnitude of any potential bias	
Interpretation	20	Give a cautious overall interpretation of results considering objectives, limitations, multiplicity of analyses, results from similar studies, and other relevant evidence	11-15
Generalisability	21	Discuss the generalisability (external validity) of the study results	
Other information			
Funding	22	Give the source of funding and the role of the funders for the present study and, if applicable, for the original study on which the present article is based	3

*Give information separately for cases and controls in case-control studies and, if applicable, for exposed and unexposed groups in cohort and cross-sectional studies.

Note: An Explanation and Elaboration article discusses each checklist item and gives methodological background and published examples of transparent reporting. The STROBE checklist is best used in conjunction with this article (freely available on the Web sites of PLoS Medicine at http://www.plosmedicine.org/, Annals of Internal Medicine at http://www.annals.org/, and Epidemiology at http://www.epidem.com/). Information on the STROBE Initiative is available at www.strobe-statement.org.